



## **Effect of $\text{TiO}_2$ addition on the properties of UPR-*DonaxGrandis* fiber composite**

**Ifa Sharmila Binti Mohamad Shah Alam**

**J20a0452**

**A report submitted in fulfilment of the requirements for the degree of the  
Bachelor of Applied Science Forest Resource Technology with Honours**

**FACULTY OF BIOENGINEERING AND TECHNOLOGY**

**UMK**

**2023**

**DECLARATION**

I declare that this thesis entitled “Effect of TiO<sub>2</sub> addition on the properties of UPR-*Donax Grandis* fiber composite” is the results of my own research except as cited in the references.

Signature : \_\_\_\_\_

Student's Name : \_\_\_\_\_

Date : \_\_\_\_\_

Verified by:

Signature : \_\_\_\_\_

Supervisor's Name : \_\_\_\_\_

Stamp : \_\_\_\_\_

Date : \_\_\_\_\_

## ACKNOWLEDGEMENT

It is with immense gratitude and heartfelt appreciation that I extend my sincere thanks to the individuals who have played pivotal roles in the successful completion of this project, contributing significantly to the enhancement of my knowledge and practical skills, particularly in the field of research.

First and foremost, I express my deepest gratitude to Dr. Mahani Yusoff, my mentor and guide throughout this project. Your expertise, guidance, and unwavering support have been invaluable, shaping not only the trajectory of this research but also fostering my personal and academic growth.

I would like to extend my thanks to assistant lab of Faculty of Bioengineering Technology, for their cooperation in helping me and giving me the support in this project. Your collaboration and insights have been instrumental in overcoming challenges and pushing the boundaries of our research endeavors.

I am grateful to my parents, Mr. Mohamad Shah Alam and Mrs. Rosliza Zakaria for their constant prayer, concern, support, patient and scarifies for my success. Finally, I want to express my gratitude to my friends and family for their unwavering encouragement and understanding throughout this academic endeavor. Your belief in my abilities has been a constant source of motivation.

In conclusion, the completion of this project was a collective effort, and I am truly fortunate to have had the support of such dedicated individuals. Each of you has played an indispensable role in my academic and personal growth, and for that, I am sincerely thankful.

## **Effect of $\text{TiO}_2$ addition on the properties of UPR-*Donax Grandis* fiber composite.**

### **ABSTRACT**

The utilization of natural fibers in polymer composite has various applications including hemp, jute, sisal, kenaf, banana, and ramie. The inner sap has not yet been employed as a reinforcing fiber due to its distinct chemical makeup. The purpose of this study was to determine the effect of titanium dioxide ( $\text{TiO}_2$ ) addition on the morphology and functional, and mechanical characteristics of unsaturated polyester resin (UPR) reinforced *Donax Grandis* inners sap fiber (DGIF) composites. UPR-DGIF-TiO<sub>2</sub> composites were produced by blending and compression molding with varying DGIF compositions (20, 25, and 30wt%) with 1wt%  $\text{TiO}_2$ . The result showed the composite with 25wt% DGIF exhibited superior tensile strength, bending strength, and hardness compared to the composites with 20wt% and 30wt% DGIF. The surface morphology revealed better and more uniform interfacial adhesion of DGIF in the UPR matrix. The chemical interaction between matrix and reinforcement was also confirmed by absorption spectra. The addition of  $\text{TiO}_2$  particles has a greater impact on improving the mechanical properties of composites with 25wt% DGIF. However, the composite with 20wt% DGIF was found to be more brittle even with added  $\text{TiO}_2$ . The optimum content of DGIF was found to be 25wt%, and the addition of 1wt%  $\text{TiO}_2$  could improve the performance of the composite. By utilizing UPR, DGIF, and  $\text{TiO}_2$  in the right ratios, it is possible to achieve a remarkable improvement in the properties of the composite. This synergistic effect can significantly enhance the overall performance and effectiveness of the material.

UNIVERSITI  
MALAYSIA  
KELANTAN

## Kesan penambahan $\text{TiO}_2$ ke atas sifat komposit UPR-Gentian *Donax Grandis*.

### ABSTRAK

Penggunaan gentian semulajadi dalam komposit polimer mempunyai pelbagai aplikasi termasuk automotif, bahan binaan, dan papan partikel. Sap dalaman jarang digunakan sebagai gentian penguat kerana komposisi kimianya yang berbeza. Tujuan kajian ini adalah untuk menentukan kesan penambahan titanium dioksida ( $\text{TiO}_2$ ) terhadap ciri-ciri morfologi, kumpulan fungsian, dan mekanikal komposit resin poliester tak jenuh (UPR) yang diperkuat dengan gentian sap dalaman *Donax Grandis* (DGIF). Komposit UPR-DGIF- $\text{TiO}_2$  dihasilkan melalui pencampuran dan pemampatan acuan dengan komposisi DGIF yang berbeza (20wt%, 25wt%, dan 30wt%) dengan 1wt%  $\text{TiO}_2$ . Komposit dengan 25wt% DGIF menunjukkan kekuatan tegangan, kekuatan lenturan, dan kekerasan yang lebih baik berbanding dengan komposit dengan 20wt% dan 30wt% DGIF. Morfologi permukaan menunjukkan lekatan antara muka yang lebih baik dan lebih seragam dari 25wt% DGIF dalam matriks UPR. Interaksi kimia antara matriks dan tulang juga disahkan oleh spektrum penyerapan. Penambahan partikel  $\text{TiO}_2$  memberi impak yang lebih besar terhadap peningkatan sifat mekanikal bagi komposit yang mempunyai 25wt% DGIF. Walau bagaimanapun, komposit dengan 20wt% DGIF didapati lebih rapuh walaupun dicampur ditambah  $\text{TiO}_2$ . Kandungan DGIF yang optimum didapati adalah 25wt%, dan penambahan 1wt%  $\text{TiO}_2$  dapat meningkatkan prestasi komposit. Dengan menggunakan UPR, DGIF, dan  $\text{TiO}_2$  dalam nisbah yang betul, adalah mungkin untuk mencapai peningkatan yang ketara dalam sifat komposit. Kesan sinergistik ini dapat meningkatkan secara signifikan prestasi dan keberkesanannya keseluruhan bahan komposit.

UNIVERSITI  
MALAYSIA  
KELANTAN

## Table of Contents

<b>DECLARATION .....</b>	<b>i</b>
<b>ACKNOWLEDGEMENT .....</b>	<b>ii</b>
<b>ABSTRACT .....</b>	<b>iii</b>
<b>ABSTRAK.....</b>	<b>iv</b>
<b>LIST OF TABLES.....</b>	<b>viii</b>
<b>LIST OF FIGURES.....</b>	<b>ix</b>
<b>LIST OF ABBREVIATIONS .....</b>	<b>x</b>
<b>CHAPTER 1.....</b>	<b>1</b>
<b>INTRODUCTION .....</b>	<b>1</b>
1.1    Background of study .....	1
1.2    Problem Statement .....	4
1.3    Objectives .....	5
1.4    Scope of study.....	5
1.5    Significant of study .....	6
1.6    Expected outcomes.....	6
<b>CHAPTER 2.....</b>	<b>7</b>
<b>LITERATURE REVIEW .....</b>	<b>7</b>
2.1    Polymer composite.....	7
2.2    Unsaturated Polyester Resin .....	8
2.3    Natural fibre as reinforced material .....	8
2.3.1 Type of natural fibre.....	10

2.3.2	Animal based fibre.....	10
2.3.3	Plant based fibre.....	11
2.3.4	<i>Donax Grandis</i> plant .....	11
2.4	Filler.....	12
2.4.1	Nanofiller.....	12
2.4.2	Nano size titanium dioxide .....	13
<b>CHAPTER 3</b>	.....	<b>15</b>
<b>MATERIALS AND METHODS</b>	.....	<b>15</b>
3.1	Materials .....	15
3.2	Methodology .....	15
3.2.1	Preparation of <i>Donax grandis</i> inner sap .....	17
3.2.2	Preparation of UPR- DGIF composite.....	17
3.2.3	Preparation of UPR- DGIF- TiO <sub>2</sub> composite.....	18
3.3	Characterizations.....	18
3.3.1	Fourier Transformed Infrared Spectroscopy .....	18
3.3.2	X-ray Diffraction .....	18
3.3.3	Hardness .....	18
3.3.4	Tensile strength.....	19
3.3.5	Bending test .....	19
3.3.6	Scanning electron microscopy (SEM) .....	20
<b>CHAPTER 4</b>	.....	<b>21</b>
<b>RESULTS AND DISCUSSION</b>	.....	<b>21</b>

4.1	X-ray diffraction .....	21
4.1.1	UPR – DGISF composite .....	21
4.1.2	UPR-TiO <sub>2</sub> and UPR – DGISF – TiO <sub>2</sub> composites.....	22
4.2	Fourier Transform Infrared Spectroscopy .....	23
4.2.1	UPR and UPR – TiO <sub>2</sub> composite.....	23
4.2.2	UPR – DGISF composites .....	25
4.2.3	UPR-DGISF-TiO <sub>2</sub> composites .....	27
4.3	Scanning electron microscope .....	28
4.3.1	UPR-TiO <sub>2</sub> composite .....	28
4.3.2	UPR -DGISF– TiO <sub>2</sub> composites.....	29
4.4	Mechanical properties .....	30
4.4.1	Tensile properties .....	30
4.4.2	Bending properties.....	32
4.4.3	Hardness .....	34
<b>CHAPTER 5.....</b>		<b>36</b>
<b>CONCLUSIONS AND RECOMMENDATIONS .....</b>		<b>36</b>
5.1	Conclusions.....	36
5.2	Recommendations.....	37
<b>REFERENCES .....</b>		<b>38</b>
<b>APPENDIX A.....</b>		<b>40</b>
<b>APPENDIX B .....</b>		<b>42</b>

**LIST OF TABLES**

<b>Table 4.1:</b> Summary of possible assignment of FTIR spectra of UPR and UPR-TiO <sub>2</sub> composite .....	34
<b>Table 4.2:</b> Summary of possible assignment of FTIR spectra of UPR-DGISF composites .....	36
<b>Table 4.3:</b> Summary of possible assignment of FTIR spectra of UPR-DGISF-TiO <sub>2</sub> composites .....	37

UNIVERSITI  
—  
MALAYSIA  
—  
KELANTAN

## LIST OF FIGURES

<b>Figure 2.3:</b> Classification of natural fibres (Hamidon et al., 2019)	9
<b>Figure 2.3.4:</b> <i>Donax Grandis</i> plant .....	11
<b>Figure 3.1:</b> Flowchart of overall experiment in this study .....	16
<b>Figure 3.2:</b> Preparation <i>Donax Grandis</i> .....	17
<b>Figure 4.1:</b> XRD pattern of UPR-30wt%DGIF composites .....	22
<b>Figure 4.2:</b> XRD patterns of a) UPR-TiO <sub>2</sub> , b) UPR-20Wt%DGIF-1wt%TiO <sub>2</sub> , c) UPR 25%wtDGIF-1wt%TiO <sub>2</sub> , and d) UPR-30DGIF-1wt%TiO <sub>2</sub> composites .	23
<b>Figure 4.3:</b> FTIR spectra of a) UPR-TiO <sub>2</sub> and b) UPR .....	24
<b>Figure 4.4:</b> FTIR spectra of a) UPR-20wt%DGIF20, b) UPR-25wt%DGIF c) UPR-30wt%DGIF composites .....	26
<b>Figure 4.5:</b> FTIR spectra a) UPR-20wt%DGIF-1wt%TiO <sub>2</sub> , b) UPR-25wt%DGIF-1wt%TiO <sub>2</sub> c) UPR-30wt%DGIF-1wt%TiO <sub>2</sub> composites .....	27
<b>Figure 4.6:</b> SEM images of UPR TiO <sub>2</sub> .....	29
<b>Figure 4.7:</b> SEM images of a) UPR-25wt%DGIF-1wt%TiO <sub>2</sub> and b) UPR-30wt%DGIF-1wt%TiO <sub>2</sub> composites at 500X magnifications.....	29
<b>Figure 4.8:</b> Tensile strength of UPR- DGIF composites.....	30
<b>Figure 4.9:</b> Tensile strength of UPR and UPR-TiO <sub>2</sub> composite .....	31
<b>Figure 4.10:</b> Tensile strength of UPR-DGIF-TiO <sub>2</sub> composites.....	32
<b>Figure 4.11:</b> Bending strength of UPR-DGIF composites at different compositions .....	32
<b>Figure 4.12:</b> Flexural strength of UPR and UPR-TiO <sub>2</sub> composite.....	33
<b>Figure 4.13:</b> Flexural strength of UPR-DGIF-TiO <sub>2</sub> composites .....	34
<b>Figure 4.14:</b> Shore D hardness of neat UPR, UPR-TiO <sub>2</sub> , UPR-DGIF and UPR-DGIF-TiO <sub>2</sub> composites .....	35

## LIST OF ABBREVIATIONS

UPR	Unsaturated polyester resins	1
NanoTiO <sub>2</sub>	Nano titanium dioxide	3
TiO <sub>2</sub>	Titanium dioxide	3
DGIF	<i>Donax grandis</i> inner sap fibre	5
FTIR	Fourier transform infrared	5
XRD	X-Ray diffraction analysis	5
SEM	Scanning Electron Microscope	5
PMs	Polymer matrix composites	7
MCs	Metal Matrix Composite	7
CMs	Ceramic Matrix Composites	7
Tg	temperatures	8
IPNs	Interpenetrating Polymer Networks	8
ATR	Attenuated total reflectance technique	18

## CHAPTER 1

### INTRODUCTION

#### 1.1 Background of study

Unsaturated polyester resins (UPR) are thermoset polymers that are used to manufacture hard components. UPR-natural fibre composite is made up of two or more separate components, which might be inorganic or organic in nature (Mahltig, 2018). The cellulose component serves as the fibre's backbone, while the inorganic component is responsible for the fibre's functionalization. These composites are utilized for structural applications because of their inexpensive cost, ease of processing, superior corrosion resistance, and availability in a range of grades. Natural fibres derived from plant-based are more economical than animal-based fibres. Plant-based fibre such as flax, hemp, bamboo, jute, and kenaf are the most common fibre used as reinforcement in UPR composite.

Reinforcing a material with fibres, offers various advantages over utilizing the material alone. While Unidirectional Fibre-Reinforced Polymer (UPR) composites have good mechanical properties on their own, adding fibres improves their mechanical performance and durability. The benefits of reinforcing UPR with fibres include increased strength, better dimensional stability, weight reduction, and design flexibility. Fibre reinforcement boosts the composite material's tensile strength, stiffness, and impact resistance substantially. The fibres distribute stress more effectively throughout the structure, reducing cracks and boosting overall structural integrity. Because of the low coefficient of thermal expansion of the reinforcement, fibre reinforced UPR composites display increased dimensional stability. This decreases the possibility of bending, shrinking, or expanding under altering environmental circumstances. Despite their improved mechanical capabilities, fibre

reinforced UPR composites are comparatively light in comparison to other materials such as metals. This weight reduction is especially helpful in industries such as aerospace and automotive, where weight savings can contribute to greater fuel efficiency and performance. Fibre reinforcing enables the mechanical properties of the composite to be tailored to meet specific application requirements.

Less studied plant-based fibre for example *Donax grandis* is interesting as their features are as strong as bamboo and kenaf. *Donax grandis* belongs to the *Marantaceae* family which was found throughout Southeast Asia. It is extensively dispersed throughout Malaysia, Thailand, Singapore, Brunei, the Philippines, Papua New Guinea, and Polynesia. They have a hollow bamboo-like stem with branching at each segment with broad and big leaves. *Donax grandis* is found in the rainforest along the river, mostly in damp areas of secondary forest and bamboo thickets. It may be grown by seed and rhizome (Ong, 2004). Medicinally leaves and roots of *Donax grandis* can be made decoction for cooling the body during fever (NurulHuda, 1999). Furthermore, the poultice of leaves and stems also can be used as an eye refreshment, and the juice from stems is effectively used against snake bites(Julius,2022). There have been several research on the extract of *Donax grandis* for medicinal purposes. However, *Donax grandis* has less been examined for its possible use in polymer composites. Additionally, the stem inner sap and hypodermis of *Donax grandis* could be extracted to serve as a fiber source for composite materials.

UNIVERSITI  
MALAYSIA  
KELANTAN

There are several natural fibers that have been used for reinforcement in composite materials. Some commonly used natural fibers include flax, hemp, jute, kenaf, sisal and others (Admin, 2022). *Donax grandis* is a type of natural fiber that is obtained from the giant reed plant. Because of its unusual characteristics, it has received interest as a potential reinforcing material. *Donax grandis* may be chosen as a reinforcement fiber for a variety of reasons, including availability and sustainability, mechanical properties, and compatibility with matrix materials. *Donax grandis* is a fast-growing plant that is abundant areas, making it a valuable natural resource. Its growing and harvesting may be controlled in a sustainable manner, making it an appealing option for environmentally aware enterprises. *Donax grandis* fibers have strong tensile strength, stiffness, and impact resistance, making them appropriate for reinforcing applications. They can improve the mechanical properties of composites.

*Donax grandis* fibers can be used with a variety of matrix materials, including thermosetting and thermoplastic polymers. This compatibility enables for good bonding between the fibers and matrix, resulting in improved overall composite qualities. However, it's important to note that the performance of natural fiber composites can be influenced by factors such as fiber processing, matrix selection, and manufacturing techniques. Therefore, thorough testing and optimization are necessary to ensure the desired performance and reliability of the composite materials.

Natural fibre and polymer matrix incompatibility is a common problem that may hinder the end product's features. UPR nanocomposites containing *Donax grandis* can be made by adding nano titanium dioxide ( $TiO_2$ ). Nano  $TiO_2$  has been employed as filler in epoxy composites because cheap production cost, greater availability, and significant mechanical and thermal qualities (Prasad, 2018). They provide greater stiffness and improve the strength of the composites by playing an important role in the fibre matrix interface for a better bonding (Sanjay et al., 2019). These particles fill the cavities within the resin and fibre which decreasing the composite total free volume. Thus, this study aims to provide an information on the effect of nano  $TiO_2$  addition in UPR-*Donax grandis* composite. A nanocomposite with unique properties and performance can also be produced.

The use of *Donax grandis* fibers alone, without any extra reinforcement, may have significant drawbacks. Here are a few things to think about: mechanical qualities,

moisture absorption, and durability. While *Donax grandis* fibers have good mechanical qualities, they may not have the same strength and stiffness as synthetic fibers like carbon or glass fibers. Natural fibers, particularly *Donax grandis* fibers, absorb more moisture than synthetic fibers. In damp or humid conditions, this can cause dimensional instability and lower mechanical qualities. Natural fibers may degrade over time, especially when exposed to extreme weather conditions or UV radiation. This can have an impact on the composite material's long-term durability and longevity.

The percentage inhibition of the nano-sized  $\text{TiO}_2$  complex was 41.51%, while the micro-sized  $\text{TiO}_2$  complex achieved a value of 27.13%, indicating that chitosan complexed with nano-sized titanium dioxide is a better radical scavenger than chitosan complexed with micro-sized titanium dioxide, which is explained by the lower particle size, resulting in a higher surface area (Enescu et al., 2020b). The unique features and advantages afforded by nanoparticles motivate the selection of nano-sized  $\text{TiO}_2$  over micro-sized  $\text{TiO}_2$  in composite materials. The advantages of using nano- $\text{TiO}_2$  are increased surface area, improved mechanical reinforcement, improved dispersion, and compatibility with matrix materials. The smaller size of nano- $\text{TiO}_2$  particles enables them to effectively transfer stress between the matrix and reinforcement phases of the composite. The high surface area and strong interfacial interaction contribute to enhanced mechanical reinforcement, including improved strength, stiffness, and impact resistance.

## 1.2 Problem Statement

Unsaturated polyester resin (UPR) composite is a common composite material choice for a variety of industrial applications especially for high strength and abrasion resistance. Plant fibres including hemp, jute, sisal, kenaf, banana, and ramie are replacing synthetic fibres in an increasing number of fibre-reinforced composites due to their sustainability. Less studied plant fibre such as *Donax grandis* could become useful for reinforcement in UPR composite. They are being less investigated or manufactured in polymer, even though it possesses the potential of other fibre plants such as bamboo and plant. In an early study on *Donax grandis* as reinforced material in starch composite, the hypodermal fibre has been extracted as source of fibre (Razali et al., 2016). The chemical composition of the inner sap fibers may differ from the

hypodermal fibers. It is likely that the inner sap fibers possess unique properties and characteristics that make them suitable for reinforcement in the UPR composite. However, the part of inner sap has been not yet further used as reinforcement fibre as they consist of different chemical composition. Thus, this study will be used the *Donax grandis* inner sap fibre (DGIF) as reinforcement in the UPR composite.

In addition, the incorporation of nano size filler into composites beneficially improve the interfacial bonding between matrix and fibre. This strategy could minimize the mechanical properties deterioration from inhomogeneous structure of the composite. This study will use  $\text{TiO}_2$  as filler because they able to disperse homogenously within the composite as well as improving the mechanical properties of the composite.

### **1.3 Objectives**

1. To prepare the UPR based composite at different DGIF loading and incorporation of  $\text{TiO}_2$  using mixing and compression molding.
2. To evaluate the effect of  $\text{TiO}_2$  addition on phase, functional group and mechanical properties of the UPR-DGIF composites.

### **1.4 Scope of study**

The purpose of this study is to produce UPR composite with DGIF with or without  $\text{TiO}_2$  addition, and to investigate the potential benefits of incorporating  $\text{TiO}_2$  fillers in the composite to improve interfacial bonding and overall mechanical properties. The properties of the UPR-DGIF composite will be investigated. UPR will be reinforced with DGIF at different compositions (20%, 25%, 30%). The  $\text{TiO}_2$  will be added as filler in various weight proportions (70: 20: 1, 70: 25: 1, 70: 30: 1, 100: 0: 1). The characterizations in this study are Fourier transform infrared (FTIR), X-Ray diffraction analysis (XRD), Scanning Electron Microscope (SEM) hardness, tensile, bending and thermal.

## 1.5 Significant of study

In this work, a new composite consisting of unsaturated polyester, *Donax Grandis* and  $TiO_2$  could offer high modulus and strength in both tensile and compression qualities. The use of DGISF in UPR and the addition of  $TiO_2$  on able to encourage the widespread use of high-performance natural fibre composites. A study was carried out to explore the effect of adding  $TiO_2$  on the characteristics of a composite material consisting of unsaturated polyester resin (UPR) and *Donax Grandis* fibre. The study sought to determine how the inclusion of  $TiO_2$  altered the mechanical, thermal, and morphological characteristics of the composite. The results of the study demonstrate UPR-*Donax grandis* fibre composites with various amounts of  $TiO_2$ .

## 1.6 Expected outcomes.

This research is anticipated to develop DGISF composites by enhancing the physical and mechanical characteristics of *Donax grandis* fibres and raising compaction pressure with  $TiO_2$  combination. The addition of  $TiO_2$  to the qualities of UPR-*Donax Grandis* fibre composite is expected to increase mechanical performance and thermal stability.  $TiO_2$  is expected to promote interfacial adhesion between the UPR matrix and the *Donax grandis* fibres. As a result, a high-quality UPR-based composite may be created.

## CHAPTER 2

### LITERATURE REVIEW

#### 2.1 Polymer composite

Composites are essentially the mixing of two or more constituent materials having differed physical or chemical properties, which when combined generate a material with attributes that differ from their original properties. Meanwhile composite reinforced natural fibres are made up of two or more separate components that might be inorganic or organic in nature (Mahltig, 2018). The matrix and fibre are the two basic components inside a composite. It is commonly developed to create unique mechanical features and enhanced efficiency characteristics that are impossible to obtain with any component material alone. Composite materials are categorised into three categories based on the organisation of the reinforcing filler: particle, fibrous, and laminate. The type of material utilised for the matrix is typically used to classify composites, that is Polymer matrix composites (PMCs), metal matrix composites (MMCs), and ceramic matrix composites (CMCs) are the basic types of composites (Carl Zweben).

PMCs are currently the most popular form of the composites due to cheap and low densities than MMCs and CMCs. PMCs can be reinforced with synthetic and natural fibres. For a sustainable application, natural fibres are preferred because abundant in nature and have characteristics such as cheap cost, lightweight, renewability, biodegradability, and high specific qualities (Girijappa et al., 2019b). Natural fibres are the most used in epoxy, polyester, and polyurethane matrices. The durability of natural fibre-based composite materials has led to an increase in their use in numerous production industries. Natural fibres are categorised according to their origin. Cotton, flax, and jute are examples of vegetable, orcellulose-based, fibres.

## 2.2 Unsaturated Polyester Resin

Unsaturated polyester resins (UPRs) are an important class of thermoset polymers. They are widely utilized because of their inexpensive cost, ease of processing, superior corrosion resistance, and availability in a range of grades. They do not produce any volatile by-products during the curing process, which makes them more appealing. They are, however, vulnerable to water, exhibit high glass transition temperatures ( $T_g$ ), and have poor fire resistance due to the polyester connections. They are not suited for advanced applications despite having robust structures and good mechanical and thermal characteristics when compared to other thermosets. As a result, they have been transformed into blends, interpenetrating polymer networks (IPNs), composites, nanocomposites, and other forms. These modifications can enhance properties such as water resistance, fire resistance, and overall performance for more advanced applications.

UPRs are referred to as “unsaturated” because they include unsaturated reactive sites along the polymer chain, often in the form of vinyl or allyl groups. Through a process called as copolymerization, these unsaturated sites can undergo crosslinking reactions with reactive monomers, most often styrene. The curing process begins with the inclusion of a crosslinking agent, most often a peroxide-based initiator. The interaction between the unsaturated polyester and the crosslinking agent produces a thermoset material with a three-dimensional network structure.

In comparison to other thermosetting resins, UPRs are comparatively affordable. They have strong flow properties and may be readily molded or sculpted into a variety of shapes utilizing processes like as casting, compression molding, or resin infusion. UPRs have good corrosion resistance, making them appropriate for use in corrosive situations. To improve their qualities and modify them for specific uses, UPRs can be changed using additives, fillers, and reinforcements.

## 2.3 Natural fibre as reinforced material

Natural fibres have attracted substantial interest as reinforcing elements in composite applications due to their numerous benefits. Improved mechanical characteristics is one of the predicted consequences and benefits of employing natural fibres as reinforced materials. Natural fibres like jute, hemp, sisal, flax, and bamboo can improve the mechanical qualities of composites. Natural fibres, when

appropriately aligned and mixed with a matrix material, can contribute to higher tensile, flexural, and impact resistance of the composite.

Over the last few decades, efforts have been made to create materials that can replace present materials while also improving mechanical and tribological properties for a number of applications. Many natural fiber-reinforced composites with superior properties have been investigated by researchers in order to replace synthetic fibres in a range of applications. As the desire for fresh materials with superior qualities than existing ones grows, researchers have experimented with many natural materials made from fruits, seeds, leaves, stems, animals, and so on (Sanjay et al., 2019).

Each form of natural fibre has its own distinct features and characteristics, such as strength, stiffness, elongation, density, and thermal properties. Natural fibre as a reinforcing material is chosen based on the application's unique needs, desired composite qualities, availability, and cost-effectiveness. It is important to note that natural fibres can be further processed or treated to improve their performance, such as through chemical treatments, mechanical processing, or surface modifications, to improve their compatibility with the matrix material and optimise the properties of the resulting composite.

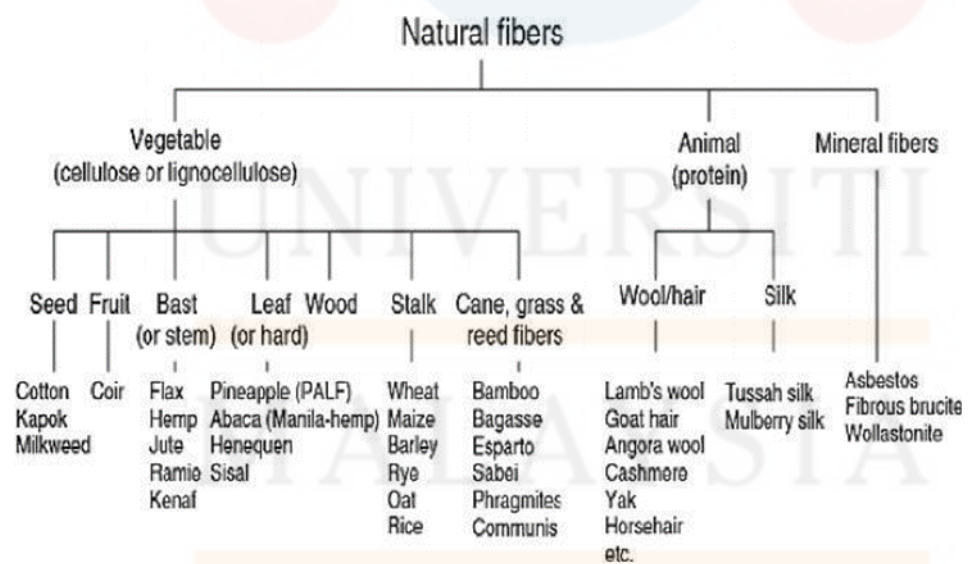


Figure 2.3 Classification of natural fibres (Hamidon et al., 2019)

### 2.3.1 Type of natural fibre

Natural fibres are classified into three categories: plant-based fibres, animal-based fibres, and mineral-based fibres (Rajak et al., 2019). Because the asbestos content in mineral-based fibres is hazardous to human health, these fibres have not been extensively researched in terms of fibre-reinforced composite materials, whereas plant-based fibres offer promising characteristics such as lower cost, biodegradability, availability, and good physical and mechanical properties.

### 2.3.2 Animal based fibre

Animal fibres are composed of structural fibrous proteins. They may be found in many different sections of an animal's body, including as hair, tissue, cartilage, skin, arteries, and muscles in mammals, and cuticles and silks in arthropods. Specific amino acids are used to build the protein in these fibres. These animal fibres are biodegradable, low density, cheap cost, widely available in a constant supply, and safe to handle (Mann et al., 2023). Renewable animal fibres offer an appealing potential for the creation of sustainable bio-composite materials. Chicken feathers and hair from other birds and animals are normally trash by-products, yet these fibres can play an important role in the future to reduce reliance on synthetic fibres (Kong, 2022). Wool and silk are animal fibres that are vital for usage in a variety of ecological applications. Furthermore, due to the presence of hydrogen bonding and the protein's hydrophobic nature, these fibres are more stable than spherical proteins. In summary, animal fibers are natural, biodegradable, and versatile materials that possess unique properties making them suitable for a wide range of applications. Their sustainability and potential for renewable production make them attractive options in the quest for more eco-friendly materials.

### 2.3.3 Plant based fibre.

Plant fibres are primarily made up of cellulose, which is frequently combined with additional components such as lignin. Cotton, hemp, jute, flax, ramie, sisal, and bagasse are examples. Plant fibres are categorised based on their origin in plants, such as bast or stem fibres, leaf fibres, and seed-hair fibre. Plant fibres are divided into primary and secondary based on their value. Primary utility plants include hemp, jute, and kenaf, whereas secondary utility plants include coir, and pineapple. Plant-derived fibres are a sort of renewable source, as well as a new generation of reinforcements and supplements for polymer-based products. These fibres are renewable, inexpensive, fully or partially recyclable, biodegradable, and ecologically beneficial materials. Their availability, low density, low cost, and good mechanical qualities make them an appealing alternative reinforcement to glass, carbon, and other synthetic fibres.

### 2.3.4 *Donax Grandis* plant

*Donax Grandis* has received interest for its possible usage in a variety of applications, including natural fibre reinforcement in composites. The plant generates long and strong fibres that may be taken from its stems. These fibres have high tensile strength, superior flexibility, and low density, making them appropriate for reinforcing materials such as polymers or matrices in composite constructions.



Figure 2.3.4 *Donax Grandis* plant

## 2.4 Filler

Fillers are solid components that are added to a matrix material to improve or attain specified qualities. When added to a matrix material, fillers can improve mechanical properties, such as stiffness and strength, increase dimensional stability, enhance thermal conductivity, or reduce cost by replacing a portion of the more expensive matrix material. These fillers might be particles, fibres, or flakes. Talc, calcium carbonate, glass fibres, and wood flour are all examples of fillers. The particle sizes of fillers generally range from a few micrometres to several hundred micrometres.

Inorganic fillers are becoming more popular in composites. Fillers not only lower the cost of composites, but they also typically increase performance that the reinforcement and resin components alone could not achieve (Zaghoul et al., 2021). By lowering organic content in composite laminates, fillers can enhance mechanical qualities such as fire and smoke resistance.

### 2.4.1 Nanofiller

For the UPR-natural fiber composites, because of the poor compatibility of UPR and natural fiber, the inhomogenous composite structure might be obtained. Nanofillers often applied in these composites to improve the interfacial bonding between matrix-reinforcement. Nanofillers are fillers with particle sizes ranging from 1 to 100 nanometers. These particles are substantially smaller in size than typical fillers. The smaller size of nano-fillers allows for greater dispersion within the matrix material, resulting in improved interfacial interactions and potentially improved overall composite performance. The choice of particle size can have an impact on the properties of the composite material. Smaller particle sizes tend to offer better dispersion and can result in improved mechanical properties, whereas larger particles may provide increased reinforcement but can affect the surface finish of the material.

Nanofillers have a high surface area-to-volume ratio due to their microscopic size. This large surface area enables for greater dispersion throughout the matrix material, resulting in better homogeneity and distribution. The increased dispersion enables efficient interfacial interactions between the nanofillers and the matrix material, resulting to improved mechanical characteristics and overall composite performance. The use of nanofillers can improve the mechanical characteristics of

composites. Because of the presence of nanofillers, the better interfacial bonding between the matrix and reinforcement can result in greater strength, stiffness, and toughness of the composite material. The tiny size of nanofillers also provides for effective load transmission between matrix and reinforcement, resulting in enhanced stress distribution and fracture propagation resistance.

Silica nanoparticles, titanium dioxide, carbon nanotubes, and clay are examples of nano-filters. Because of their small size and high surface area-to-volume ratio, nano-filters have distinct qualities and characteristics (Cazan et al., 2021). When mixed into a matrix material, they can give better mechanical strength, improved barrier characteristics, increased thermal stability, and unique optical or electrical capabilities.

#### **2.4.2 Nano size titanium dioxide**

Titanium dioxide ( $TiO_2$ ) is the element titanium's natural oxide. From a commercial standpoint,  $TiO_2$  is available in two main forms that differ in crystal structure: anatase and rutile.  $TiO_2$  may be synthesised in a variety of morphologies, including nanoparticles, nanowires, nanotubes, and mesoporous structures. Because of its increased physical and mechanical qualities,  $TiO_2$  is utilised as a filler in many polymeric matrices.

Many investigations found that  $TiO_2$ -filled polymeric nanocomposites had higher mechanical strength and modulus than the pristine-base matrix. This is because the internal structure of polymer nanocomposites containing nano- $TiO_2$  has a large effect on their mechanical characteristics (Cazan et al., 2021b). The usage of  $TiO_2$  in polymer-natural fibre nanocomposites has various possible advantages and capabilities.  $TiO_2$  nanoparticles can improve the mechanical characteristics of polymer-natural fibre composites by strengthening the matrix and enhancing stiffness, strength, and toughness. This reinforcing effect can result in increased load-bearing capacity and resistance to deformation.  $TiO_2$  nanoparticles can also improve the thermal stability of polymer-natural fibre composites, making them more resistant to high temperatures. This is especially advantageous in situations where the nanocomposite must tolerate high temperatures without considerable deterioration.  $TiO_2$  nanoparticles can alter the optical characteristics of polymer-natural fibre nanocomposites, such as transparency and opacity. This makes  $TiO_2$  excellent for applications requiring optical control, such as films, coatings, or optical devices.

Nano-sized titanium dioxide (nano-TiO<sub>2</sub>) particles and non-nano TiO<sub>2</sub> particles are both versions of the chemical compound titanium dioxide (TiO<sub>2</sub>), but their particle size and characteristics differ dramatically. Nano-TiO<sub>2</sub> refers to titanium dioxide particles of nanoscale dimensions (usually fewer than 100 nanometers), whereas non-nano TiO<sub>2</sub> consists of bigger particles, typically in the micrometer range. Their physical traits and conduct are the primary distinguishing factors. Because of their tiny size, nano-TiO<sub>2</sub> particles have distinct traits such as increased surface area, higher reactivity, and changed optical properties when compared to non-nano counterparts. Nano-TiO<sub>2</sub>'s properties make it appealing for a variety of applications, including sunscreen, cosmetics, and catalysts.

UNIVERSITI  
MALAYSIA  
KELANTAN

## CHAPTER 3

### MATERIALS AND METHODS

#### 3.1 Materials

*Donax Grandis* plants were harvested at Agro Park, Universiti Malaysia Kelantan, Jeli Campus, Kelantan, Malaysia. The unsaturated polyester resin (UPR) was purchased from Rivertex Sdn Bhda and  $\text{TiO}_2$  was purchased from Sigma Aldrich.

#### 3.2 Methodology

The overall experiment in this study is shown in Figure 3.1. This study was involves of three main stages. First, the preparation of *Donax grandis* fiber. Then followed by preparation of UPR- *Donax grandis* inner sap fibres (DGIF) composite and lastly preparation of UPR- DGIF-  $\text{TiO}_2$  nanocomposite.

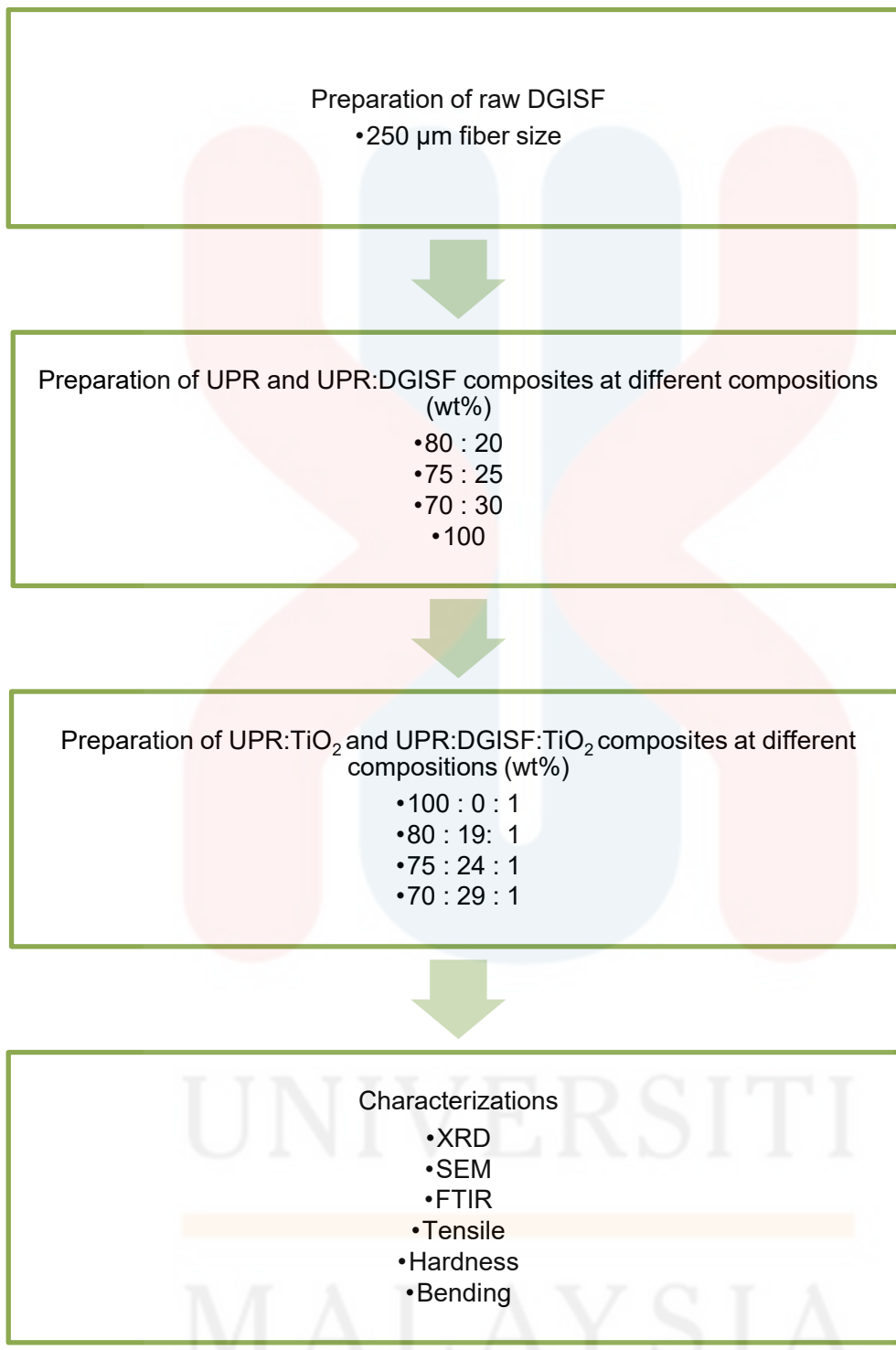


Figure 3.1: Flowchart of overall experiment in this study

### 3.2.1 Preparation of *Donax grandis* inner sap

The *Donax grandis* stem was cut using a knife. Then, the inner sap was extracted. To eliminate impurities and pollutants, the extracted DGISF were washed and dried for 48 hours under room temperature. Then, the DGISF size was ground using a commercial blender and sieved at 250  $\mu\text{m}$  using a steel siever.



Figure 3.2: Preparation *Donax Grandis*

### 3.2.2 Preparation of UPR- DGISF composite

The UPR was prepared using different contents of DGISF (20, 25, and 30wt%). The UPR was mixed with DGISF at 100 rpm using a stirrer. Then, the composite was transferred to a 15 cm x 15 cm stainless steel mold and pressed at 100 MPa using a compression mold machine. The composite was then dried for 24 hours at room temperature.

### 3.2.3 Preparation of UPR- DGISF- TiO<sub>2</sub> composite

The TiO<sub>2</sub> was added as a filler in various weight proportions (70: 20: 1, 70: 25: 1, 70: 30: 1, 100: 0: 1). The DGISF was added to the UPR in a stainless-steel mold (15 cm x 15 cm x 0.1 cm). Then, TiO<sub>2</sub> particles were mixed into the UPR using a stirrer until uniform dispersion was achieved. The composite was pressed at 100 MPa. The composite mixture was placed in a vacuum chamber to remove any trapped air or foam, ensuring that the vacuum was on long enough to ensure complete degassing. Then, the UPR was cured at 80°C for effective consolidation of the composite.

## 3.3 Characterizations

### 3.3.1 Fourier Transformed Infrared Spectroscopy

The functional groups of the composite were analyzed using attenuated total reflectance technique (ATR)-based Thermo Scientific TM iN10 Fourier Transformed Infrared Spectroscopy (Thermo Fisher Scientific Inc., MA, USA). Sixteen scans were taken from 400 to 4000 cm<sup>-1</sup> with a resolution of 2 cm<sup>-1</sup>. Spectral outputs were recorded in the transmittance mode as a function of wavenumber. Samples of UPR-TiO<sub>2</sub>, UPR-DGISF, and UPR-DGISF-TiO<sub>2</sub> composites were cut in 10 mm x 10 mm x 3 mm size and tested.

### 3.3.2 X-ray Diffraction

X-ray Diffraction (XRD) is a widely used analytical technique that provides valuable information about the crystallographic structure, phase composition, and preferred orientation of crystalline materials. The Bruker D2 Phaser X-ray Diffraction (XRD) was used to characterize the composite for phase identification. A step size of 0.02° with the 2θ angle of 20° to 90° was used. The DIFFRAC.EVA software was used to determine phase identification and perform analysis on the XRD patterns of the composite. Samples tested were cut into 10 mm x 10 mm x 3 mm dimensions.

### 3.3.3 Hardness

The microhardness of a coated welded sample and a composite film was tested with a Shore D Durometer, following the ASTM D2240 standard. Five readings were made on the specimen's center part, and the mean hardness was calculated from those. The hardness measurements acquired with the Shore D Durometer aided in determining the compatibility and quality of the coated welded sample and composite

film, providing significant information for material selection, quality control, and performance assessment. The samples for this test were cut into 10mm x 10mm x 3mm dimensions, and the measurements were done at one point of the material and repeated at another point.

### **3.3.4 Tensile strength**

Mechanical testing was used to characterize composite qualities. Tensile, flexural, and impact testing were performed on the composite specimens using established testing procedures. Tensile testing of composites was generally in the form of basic tension or flat-sandwich tension testing in accordance with standards such as ISO 527-4, ISO 527-5, ASTM D 638, ASTM D 3039, and ASTM C 297 (Saba et al., 2019). The tensile strength and flexural strength were determined.

The test consisted of delivering an axial load or force on a material specimen, often in the form of a standardized test specimen with predetermined dimensions. The tension was gradually applied, stretching the specimen until it fractured or failed. The applied force and the consequent elongation or deformation of the specimen were recorded during the test using ASTM D638. The specimen's dimensions were 150mm x 20mm x 3mm, and a uniaxial load was applied via both ends. The universal testing equipment Testomeric equipment 0500-11213 was used for this test, with a crosshead speed of 5 mm/min.

### **3.3.5 Bending test**

Bending tests involved extending a length of material across a span and pressing down along the span to bend it until it failed. Bending tests determined a material's elastic modulus of bending, flexural stress, and flexural strains. The specimen for the bending test was cut from the necessary panels using ASTM D7264 (American Standard Testing and Materials) (Iqbal et al., 2023). The specimen's dimensions were 150mm x 20mm x 3mm, and a uniaxial stress was applied from both ends. This test was conducted using the universal testing equipment Testomeric equipment 0500-11213 at a crosshead speed of 5 mm/min. The test was terminated when the sample began to break.

### 3.3.6 Scanning electron microscopy (SEM)

The scanning electron microscope (SEM) was one of the most often used tools for investigating and analysing micro- and nanoparticle imaging characterization of solid materials. The surface of the UPR-DGISF-TiO<sub>2</sub> composite was investigated using a scanning electron microscope. The sample was cut in cross-section to display the adhesive line, reflecting the interaction between the adhesive and the substrate as well as penetration into the composite material. The sample was examined by placing it on a SEM holder using double-sided tape. The test was performed at 5kV at magnifications ranging from 500x to 1000x.

UNIVERSITI  
[redacted]  
MALAYSIA  
[redacted]  
KELANTAN

## CHAPTER 4

### RESULTS AND DISCUSSION

#### 4.1 X-ray diffraction

X-ray diffraction (XRD) is a method for analyzing materials' crystal structure. XRD can give useful information regarding the organization of crystalline structures as well as the arrangement of atoms inside unsaturated polyester resin (UPR)-based composites. XRD can assist detect and quantify the existence of crystalline phases in composite materials including UPR as the matrix.

##### 4.1.1 UPR – DGIF composite

The XRD patterns of UPR-30 wt% DGIF is shown in Figure 4.1. The major diffraction peaks are centered around  $21^\circ$  to  $23^\circ$ . The peaks correspond to the crystalline part of cellulose found in DGIF. It is important to note that UPR is a thermosetting polymer with an amorphous (non-crystalline) structure and so may not be highly crystalline. The diffraction peaks in this region correspond to cellulose's crystal lattice structure. The intensity and position of these peaks can reveal the degree of crystallinity. DGIF may present in common crystalline phases of UPR-based composites.

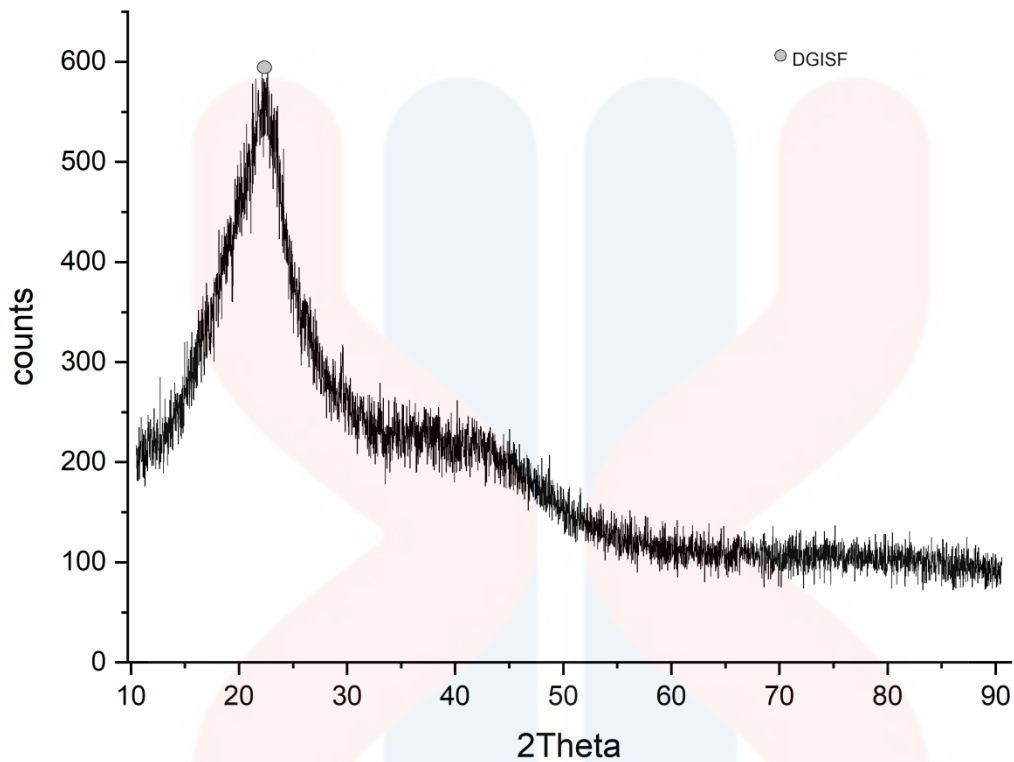


Figure 4.1: XRD pattern of UPR-30wt%DGIF composites

#### 4.1.2 UPR-TiO<sub>2</sub> and UPR – DGIF – TiO<sub>2</sub> composites

The diffraction peak value of crystalline region and amorphous region are presented in Figure 4.2. There is no sharp peak was found in Figure 4.2 a) (UPR-TiO<sub>2</sub> but there were only a few visible points that are on 24.76° and 27.30° that are corresponding to TiO<sub>2</sub>. This diffraction conforming to crystalline phase of TiO<sub>2</sub> in anatase phase which at 25.27° and 25.68°. The peaks of 25.68° at Figure 4.2 (c) correspond to TiO<sub>2</sub> anatase, new broad peaks of cellulose were visible at 11.11° with increasing the fiber of DGIF. The peak of (d) in the Figure 4.2 is the same with the (c) that is 25.68° corresponds to anatase of TiO<sub>2</sub>. Observe the peaks in the XRD pattern that match to TiO<sub>2</sub> crystallographic planes. The locations and intensities of these peaks can aid in determining the crystal phases contained in the composite. Anatase, rutile, and brookite are common TiO<sub>2</sub> crystal phases. Peak broadening can also reveal information about the size of TiO<sub>2</sub> nanoparticles.

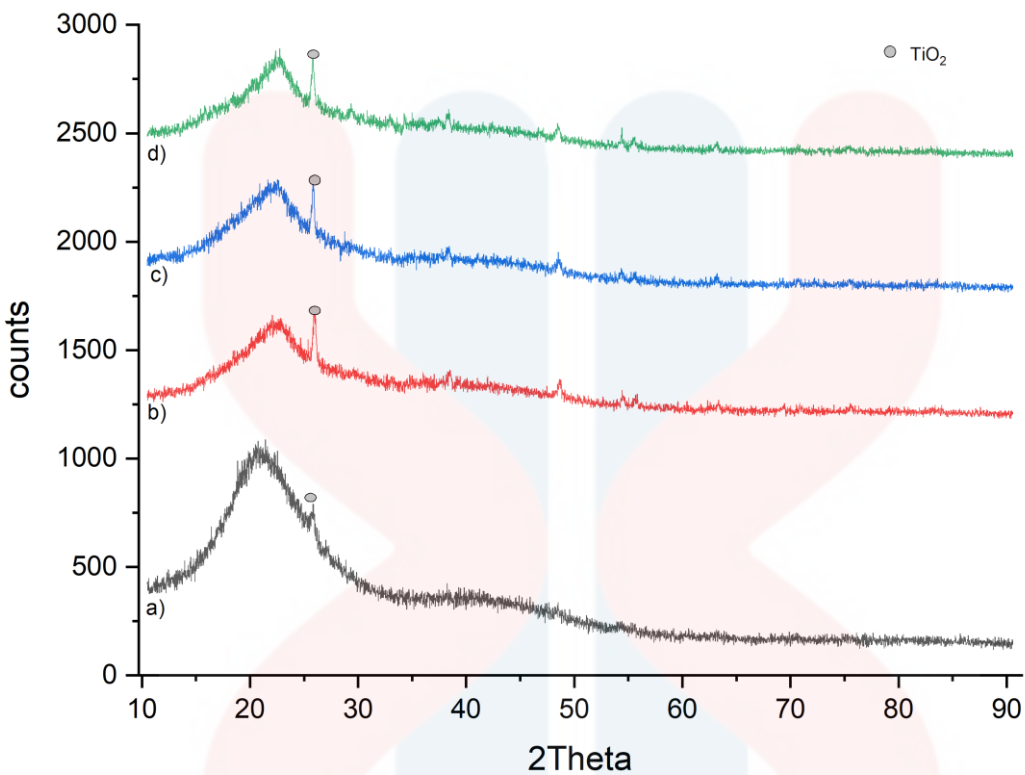


Figure 4.2: XRD patterns of a) UPR-TiO<sub>2</sub>, b) UPR-20Wt%DGIF-1wt%TiO<sub>2</sub>, c) UPR-25%wtDGIF-1wt%TiO<sub>2</sub>, and d) UPR-30DGIF-1wt%TiO<sub>2</sub> composites

## 4.2 Fourier Transform Infrared Spectroscopy

Fourier Transform Infrared Spectroscopy (FTIR) is a technique for determining a material's molecular composition by measuring its infrared light absorption. This technique was used to understand the impact of DGIF and TiO<sub>2</sub> on the molecular composition in the UPR matrix. The spectra obtained for UPR, UPR-TiO<sub>2</sub>, UPR-DGIF, and UPR-DGIF-TiO<sub>2</sub> composite were evaluated using absorption bands ranging from 4000 to 400 cm<sup>-1</sup>.

### 4.2.1 UPR and UPR – TiO<sub>2</sub> composite

Figure 4.4 shows the FTIR spectra of UPR and UPR-TiO<sub>2</sub>. Both UPR-TiO<sub>2</sub> and UPR spectra show a wide absorption peak about 3500 cm<sup>-1</sup>, suggesting the presence of O-H stretching vibrations. These vibrations are often associated with hydroxyl groups, perhaps from hydroxyl-containing substances such as alcohols, phenols, or carboxylic acids (Table 4.1). However, the peak intensity in UPR-TiO<sub>2</sub> was somewhat lower than in UPR, indicating a possible interaction between the TiO<sub>2</sub>

nanoparticles and the hydroxyl groups in the resin matrix. The bands seen at  $2930\text{ cm}^{-1}$  are C-H stretching vibrations of alkanes, especially the C=C stretching mode. The absorption peaks in this area indicate the existence of carbon-carbon double bonds, which are typical of alkenes and aromatic compounds.

The minor change in wavenumber between UPR and UPR-TiO<sub>2</sub> composite reflect chemical differences or the presence of TiO<sub>2</sub> in UPR-TiO<sub>2</sub>. Carbonyl peaks about  $1720\text{ cm}^{-1}$  correspond to C=O stretching vibrations in ketones. The closeness in peak locations and intensities between UPR-TiO<sub>2</sub> and UPR implies that the addition of TiO<sub>2</sub> had no substantial effect on the carbonyl group content of the resin matrix. The spectra also show peaks about  $1258\text{ cm}^{-1}$ , which correspond to C=C stretching vibrations of alkene groups. Furthermore, the bands detected at  $743\text{ cm}^{-1}$  correspond to the C-H bending vibrations commonly associated with benzene rings aromatic molecule. Overall, the absorption peaks for UPR and UPR-TiO<sub>2</sub> composite are comparable, indicating the existence of similar functional groups. The tiny broadening in peak wavenumbers at 699 and  $742\text{ cm}^{-1}$  might be related to the interaction between UPR and TiO<sub>2</sub> in the UPR-TiO<sub>2</sub> composite.

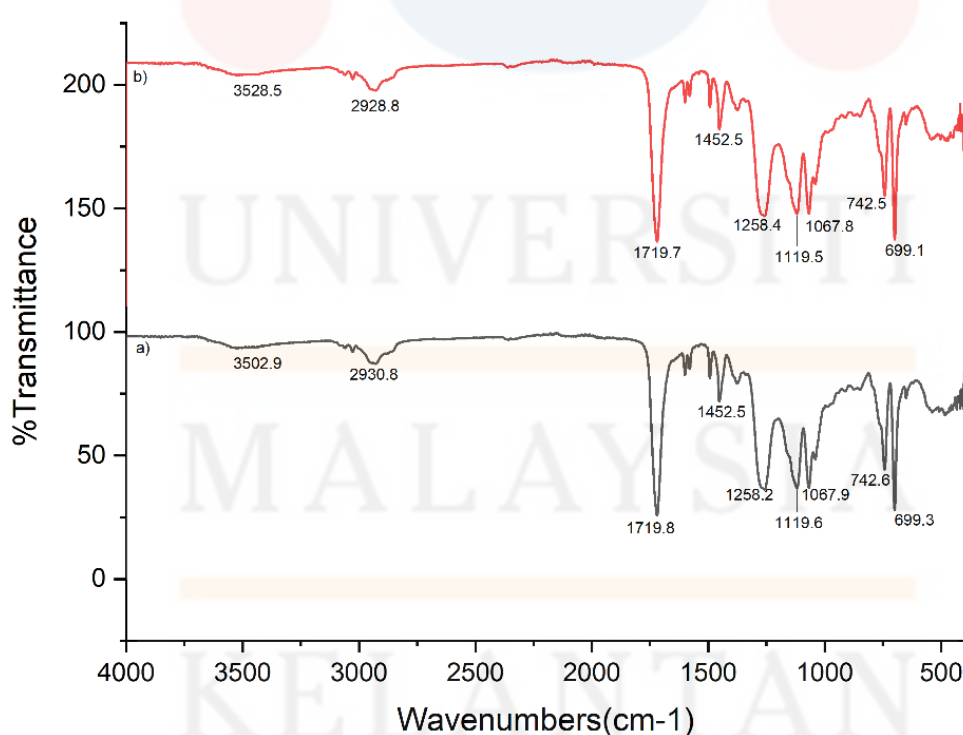


Figure 4.3: FTIR spectra of a) UPR-TiO<sub>2</sub> and b) UPR

Table 4.1: Summary of possible assignment of FTIR spectra of UPR and UPR-TiO<sub>2</sub> composite

Possible assignments	UPR-TiO <sub>2</sub>	UPR
O-H stretching	3502.9	3528.5
C=C stretching(alkanes)	2930.8	2928.8
C=O stretching(ketones)	1719.8	1719.7
C=C stretching(alkanes)	1258.2	1258.4
C-H bending(benzene)	742.6	742.5

#### 4.2.2 UPR – DGIF composites

Figure 4.4 shows the FTIR spectra of UPR-DGIF at various compositions. Table 4.1 presents summary of possible assignment of FTIR spectra of UPR-DGIF composites. N-H bonding was detected at 3420 cm<sup>-1</sup>, confirming the existence of stretching vibrations. However, the peak intensity decreased somewhat when the concentration of DGIF grew from 20% to 30%, indicating that the modifier may have an effect on the hydrogen bonding network inside the resin matrix. The detected bands at 2925 cm<sup>-1</sup> correspond to C-H stretching vibrations of alkanes, especially the C=C stretching mode. Interestingly, when DGIF concentration increased, peak locations shifted somewhat downward, indicating a possible interaction between the modifier and the resin matrix's alkane chains. Carbonyl group peaks at 1720 cm<sup>-1</sup> correlate to C=O stretching vibrations in ketones. The peak locations varied little with DGIF concentration, indicating that the presence of the modifier had no substantial effect on the carbonyl group composition of the resin matrix. The spectra also show peaks about 1258 cm<sup>-1</sup>, indicating C=C stretching vibrations of alkene groups.

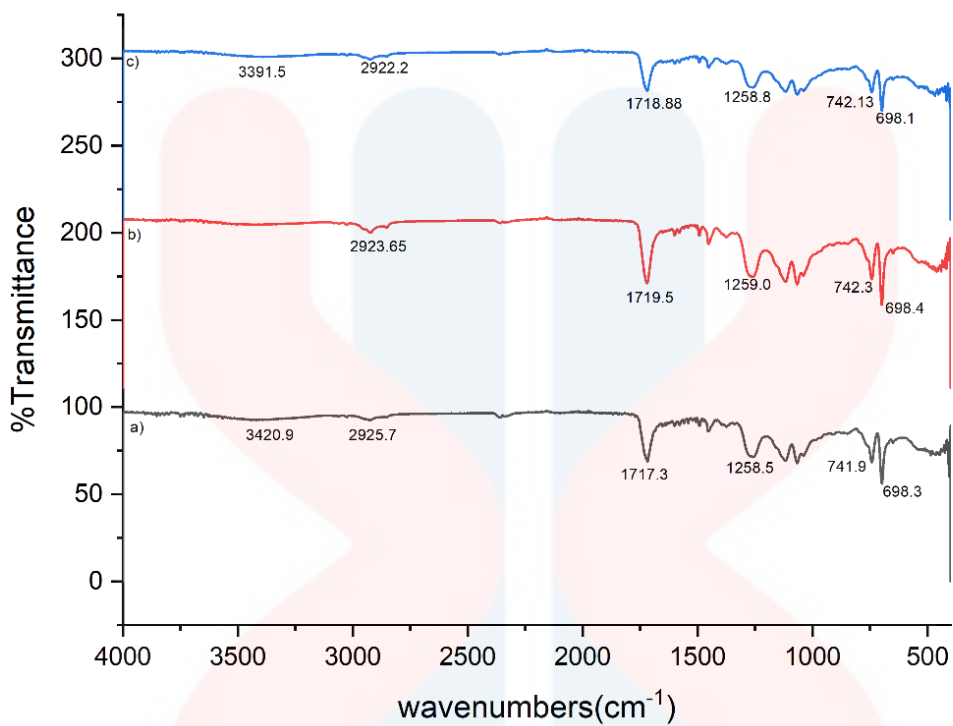


Figure 4.4: FTIR spectra of a) UPR-20wt%DGIF20, b) UPR-25wt%DGIF c) UPR-30wt%DGIF composites

Table 4.2: Summary of possible assignment of FTIR spectra of UPR-DGISF composites

Possible assignments	UPR-20wt%DGIF	UPR-25wt%DGIF	UPR-30wt%DGIF
N-H stretching	3420.9	-	3391.5
C=C stretching(alkanes)	2925.7	2923.6	2922.2
C=O stretching(alkanes)	1717.3	1719.5	1718.8
C=C stretching(alkanes)	1258.5	1259.0	1258.8
C-H bending(benzene)	741.9	742.3	742.1

The peak locations, like the carbonyl groups, remained reasonably stable as the concentration of DGIF varied. The detected bands about  $742\text{ cm}^{-1}$  correspond to the C-H bending vibrations associated with benzene rings. The peak locations, like the other functional groups, showed little modification with altering DGIF concentration, indicating that the aromatic structures within the resin matrix were mostly unaffected by the modifier's presence. In general, the FTIR analysis demonstrated that, while peak intensities and locations varied somewhat with DGIF concentration, the overall

structural composition of UPR-DGISF composites remained generally consistent across formulations.

#### 4.2.3 UPR-DGISF-TiO<sub>2</sub> composites

Figure 4.5 shows the FTIR spectra of UPR-DGISF-TiO<sub>2</sub> at different compositions. Table 4.1 presents summary of possible assignment of FTIR spectra of UPR-DGISF-TiO<sub>2</sub> composites. The N-H stretching frequencies are recorded at 3392.9 cm<sup>-1</sup> for UPR-20wt%DGIF-1wt%TiO<sub>2</sub>, 3397.2 cm<sup>-1</sup> for UPR-25wt%DGIF-1wt%TiO<sub>2</sub>, and 3396.3 cm<sup>-1</sup> for UPR-30wt%DGIF-1wt%TiO<sub>2</sub>. These results indicate the existence of amino or amide groups in the compounds. The C=C stretching (alkanes) peaks are observed at 2925.1 cm<sup>-1</sup> for UPR-20wt%DGIF-1wt%TiO<sub>2</sub>, 2932.6 cm<sup>-1</sup> for UPR-25wt%DGIF-1wt%TiO<sub>2</sub>, and 2926.7 cm<sup>-1</sup> for UPR-30wt%DGIF-1wt%TiO<sub>2</sub> composites. These frequencies suggest the existence of carbon-carbon double bonds, which are commonly seen in alkanes.

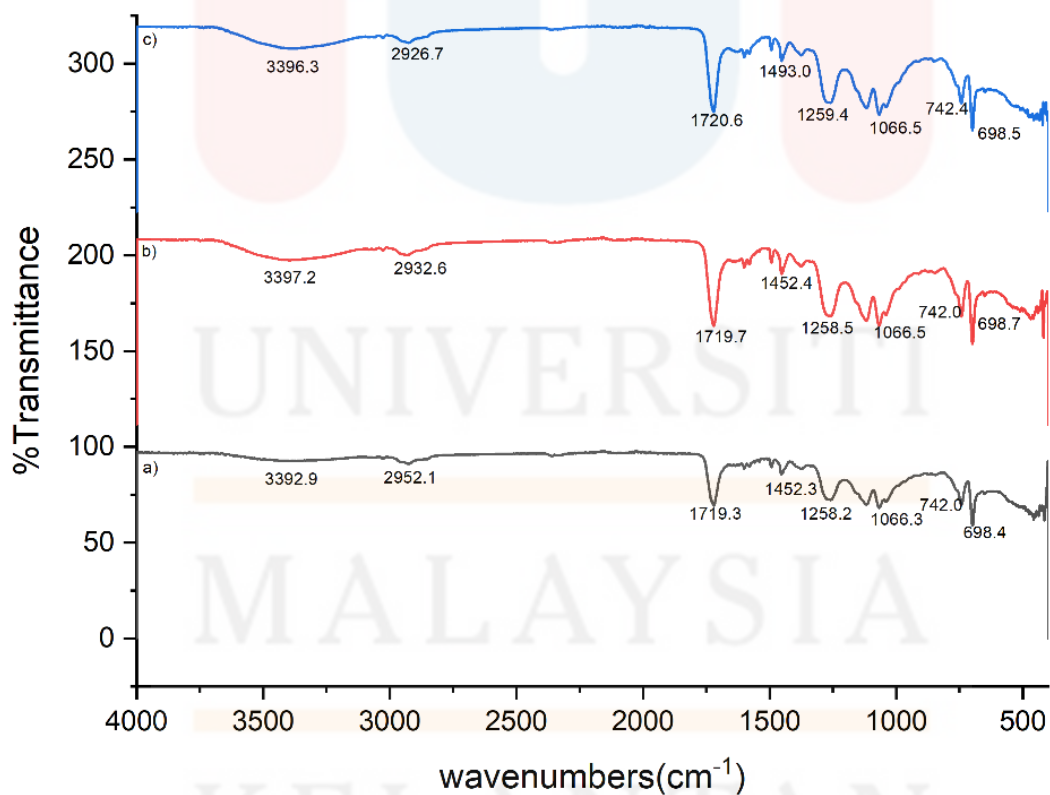


Figure 4.5: FTIR spectra a) UPR-20wt%DGIF-1wt%TiO<sub>2</sub>, b) UPR-25wt%DGIF-1wt%TiO<sub>2</sub> c) UPR-30wt%DGIF-1wt%TiO<sub>2</sub> composites

Table 4.3: Summary of possible assignment of FTIR spectra of UPR-DGISF-TiO<sub>2</sub> composites

Possible assignments	UPR-DGISF-TiO <sub>2</sub> 20	UPR-DGISF-TiO <sub>2</sub> 25	UPR-DGISF-TiO <sub>2</sub> 30
N-H stretching	3392.9	3397.2	3396.3
C=C stretching (alkanes)	2925.1	2932.6	2926.7
C=O stretching(benzoate)	1719.3	1719.7	1720.6
C=O stretching(benzoate)	1258.2	1258.5	1259.4
C-H bending	742.0	742.0	742.4

The C=O stretching (benzoate) bands are seen at 1719 to 1720 cm<sup>-1</sup> for composite containing TiO<sub>2</sub> which also similar to that of UPR-DGISF composites. These frequencies correlate to the stretching vibrations of carbonyl groups found in benzoates. C-H bending frequencies were identified at 742.0 cm<sup>-1</sup>. These peaks represent the bending vibrations of carbon-hydrogen bonds, which might be ascribed to diverse chemical structures found in the samples. The absorption peak of UPR-DGISF-TiO<sub>2</sub> composites at 648 to 742 cm<sup>-1</sup> become broader when compared to UPR-DGISF composites within the same range with addition of TiO<sub>2</sub> particles. Overall, the FTIR analysis indicates that all the composites have similar functional groups, implying equivalent chemical compositions.

### 4.3 Scanning electron microscope

#### 4.3.1 UPR-TiO<sub>2</sub> composite

Figure 4.6 shows the SEM images of UPR-TiO<sub>2</sub> composite. The analysis of fractured surfaces through SEM images provides valuable insights into the microstructural characteristics and mechanical properties of composite materials. In the examination of UPR reinforced with TiO<sub>2</sub>, the fractured surfaces reveal the interactions between the polymer matrix and the TiO<sub>2</sub> particles under stress. The fractured surfaces display distinctive features that offer clues about the material's fracture mechanism and overall toughness. Micrographs show the dispersion of TiO<sub>2</sub> particles within the resin matrix, illustrating the extent of particle-matrix bonding. Moreover, there are many spots and clumpy TiO<sub>2</sub> particles in the UPR matrix.

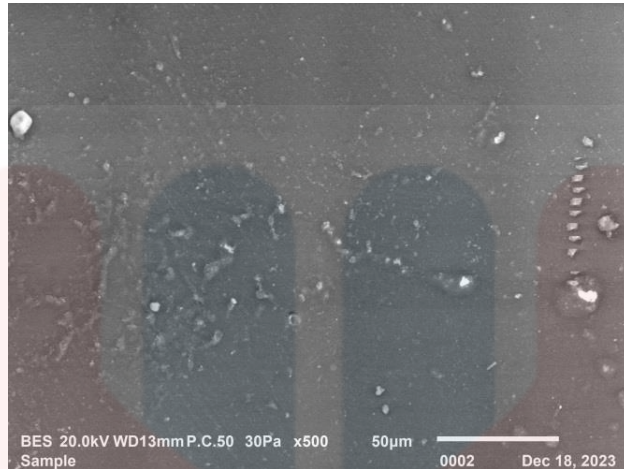


Figure 4.6: SEM images of UPR TiO<sub>2</sub>

#### 4.3.2 UPR -DGIF-TiO<sub>2</sub> composites

Figure 4.7 shows the SEM images of UPR-DGIF-TiO<sub>2</sub> composites at different compositions. The morphology reveals the intricate details of the cross-sectional view, showcasing the distribution and alignment of DGIF along with the incorporation of TiO<sub>2</sub> within the UPR matrix. The interaction between the polymer matrix, natural fibers, and TiO<sub>2</sub> particles is critical for determining the composite's mechanical properties and overall performance.

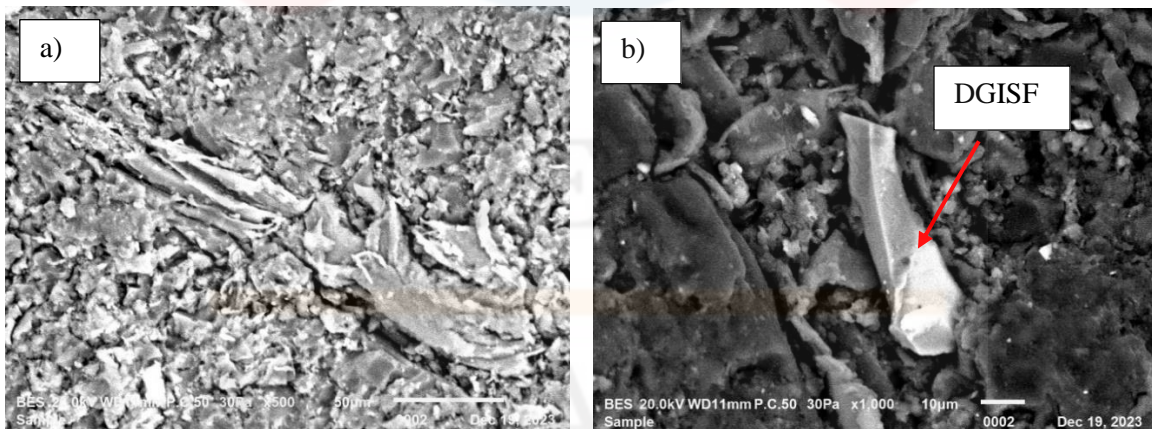


Figure 4.7: SEM images of a) UPR-25wt%DGIF-1wt%TiO<sub>2</sub> and b) UPR-30wt%DGIF-1wt%TiO<sub>2</sub> composites at 500X magnifications

## 4.4 Mechanical properties

### 4.4.1 Tensile properties

Figure 4.8 shows the tensile strength of UPR-DGISF composites. UPR-DGISF 25 has the maximum tensile strength of 7.48 MPa, followed by UPR-20wt%DGIF (6.77 MPa) and UPR-30wt%DGIF (6.48 MPa) composite. UPR-25wt%DGIF has the highest tensile qualities, most likely due to more uniform dispersion or better fiber alignment, which results in increased strength. Better interface adhesion improves the composite material's overall strength. Although UPR-30wt%DGIF contains the most fiber, its tensile strength is lower than UPR-25wt%DGIF as result of potential mixing inconsistencies.

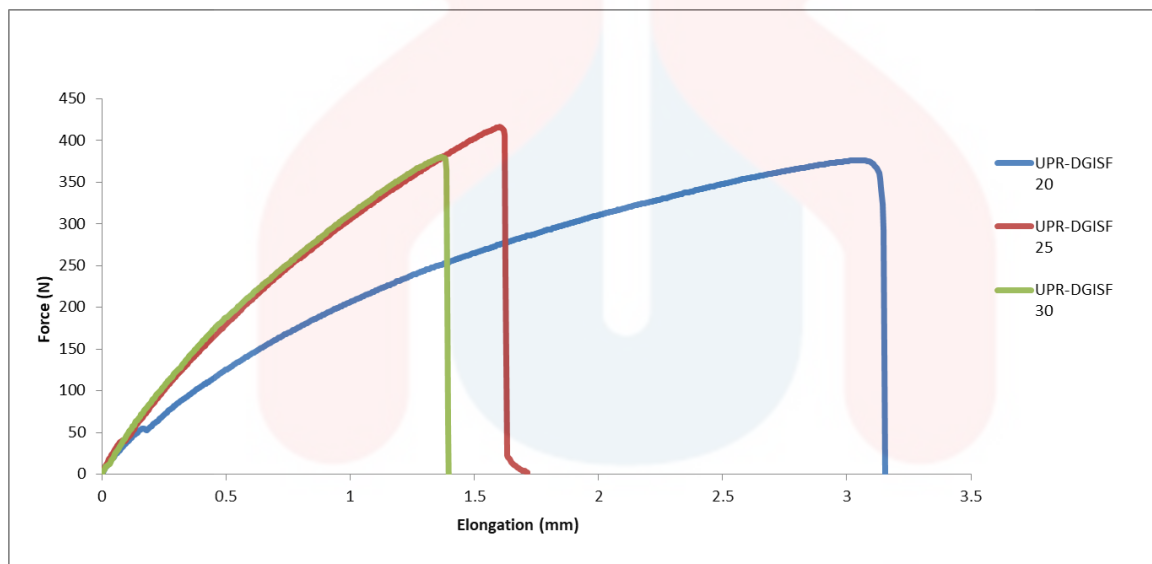


Figure 4.8: Tensile strength of UPR- DGIF composites

Figure 4.9 shows the tensile strength of UPR and UPR-TiO<sub>2</sub> composite. The tensile strength of neat UPR is greater than that of composite UPR-TiO<sub>2</sub> composite, which 40.06 MPa and 22.53 MPa, respectively. The purpose of adding TiO<sub>2</sub> is to enhance the mechanical characteristics of the mix, such as compression strength and modulus, while still maintaining adequate ductility. The TiO<sub>2</sub> powder combination composite's compressive strength is lowered. This might be because the TiO<sub>2</sub> particles are not dispersed optimally, leading in lower compressive strength.

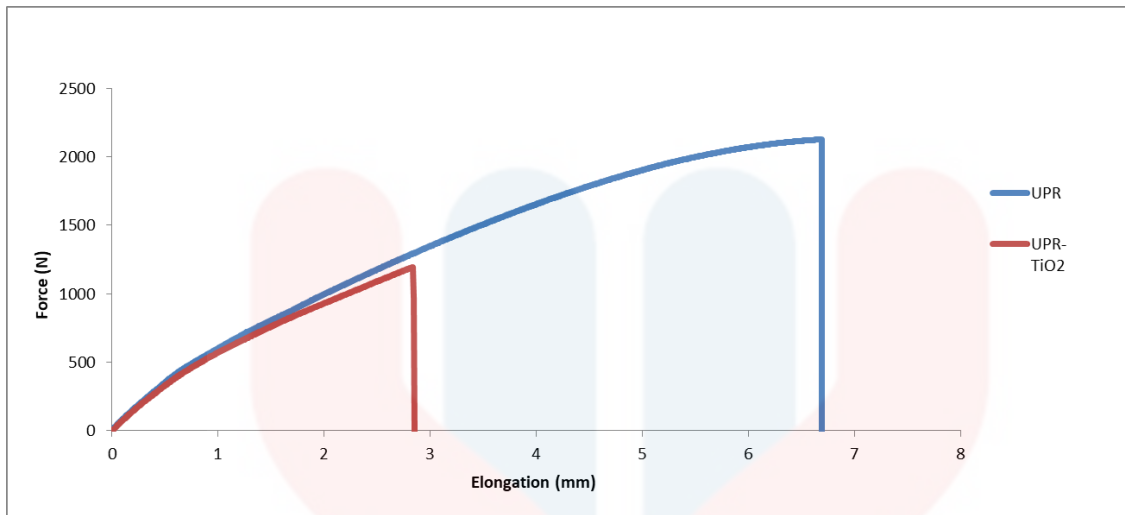


Figure 4.9: Tensile strength of UPR and UPR-TiO<sub>2</sub> composite

The tensile strength of UPR-DGISF-TiO<sub>2</sub> composites at different compositions is presented in Figure 4.10. The UPR-25wt%DGIF-1wt%TiO<sub>2</sub> composite has the highest tensile strength when compared to the other composites. Meanwhile, a slight reduction of tensile strength also was found in UPR-30wt%DGIF-1wt%TiO<sub>2</sub> composite. In these both composites, TiO<sub>2</sub> particles give an impact on the strength of the composites. However, TiO<sub>2</sub> particles in UPR-25wt%DGIF-1wt%TiO<sub>2</sub> composite might help in more evenly distributed and interactions between DGIF and UPR. The composite with lower content of DGIF (20wt%) are more prone to be brittle than the UPR-25wt%DGIF-1wt%TiO<sub>2</sub> and UPR-30wt%DGIF-1wt%TiO<sub>2</sub> composites. The combination of UPR, DGIF, and TiO<sub>2</sub> in a certain ratio can provide a synergistic effect in which the different components complement one another, resulting in a composite material with greater tensile strength. The distribution and dispersion of TiO<sub>2</sub> particles in the composite have a considerable impact on its mechanical characteristics.

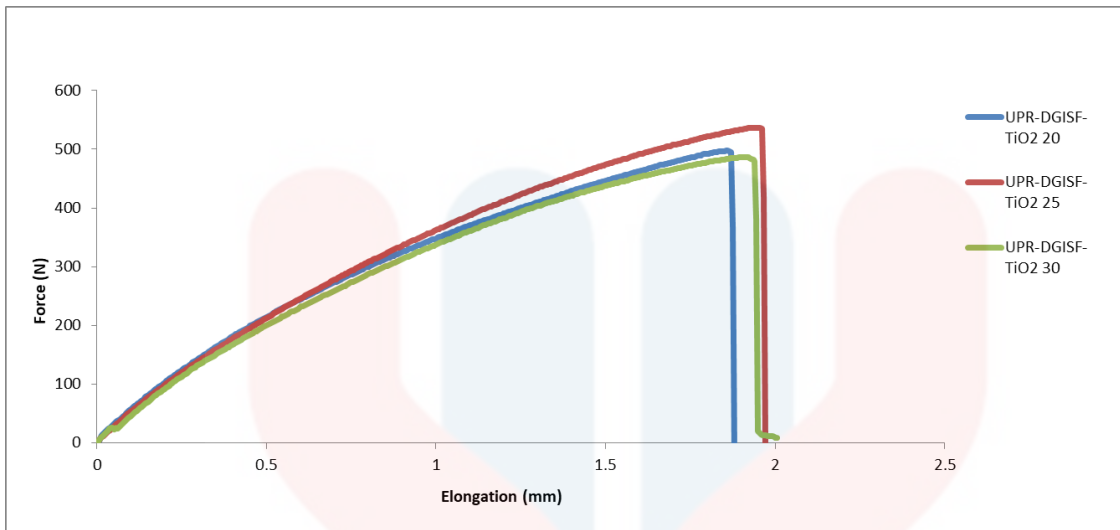


Figure 4.10: Tensile strength of UPR-DGISF-TiO<sub>2</sub> composites

#### 4.4.2 Bending properties

Figure 4.11 shows the bending strength of UPR-DGISF composites at different compositions. The bending strength of UPR-25wt%DGIF was observed greater than that of UPR-20wt%DGIF and UPR-30wt%DGIF composites. The flexural strength of UPR- UPR-25wt%DGIF and UPR-30wt%DGIF is comparable since both have a high fiber content and better interaction (Figure 4.7). Better adhesion can help to improve stress transmission between the matrix and the fibers, boosting the composite material's overall strength.

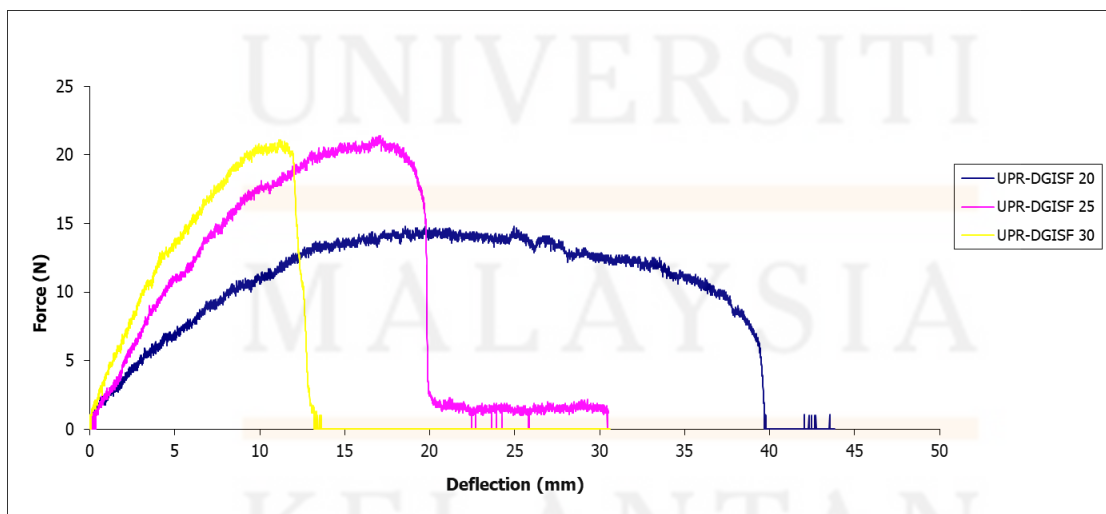


Figure 4.11: Bending strength of UPR-DGISF composites at different compositions

Figure 4.12 presents the bending strength of UPR and UPR-TiO<sub>2</sub> composite. UPR is highly flexible compared to UPR-TiO<sub>2</sub> composite. The addition of TiO<sub>2</sub> to the UPR matrix significantly reduced the flexural strength of UPR. TiO<sub>2</sub> particles might clustered together rather than being evenly dispersed, they might generate weak areas in the material, diminishing overall strength.

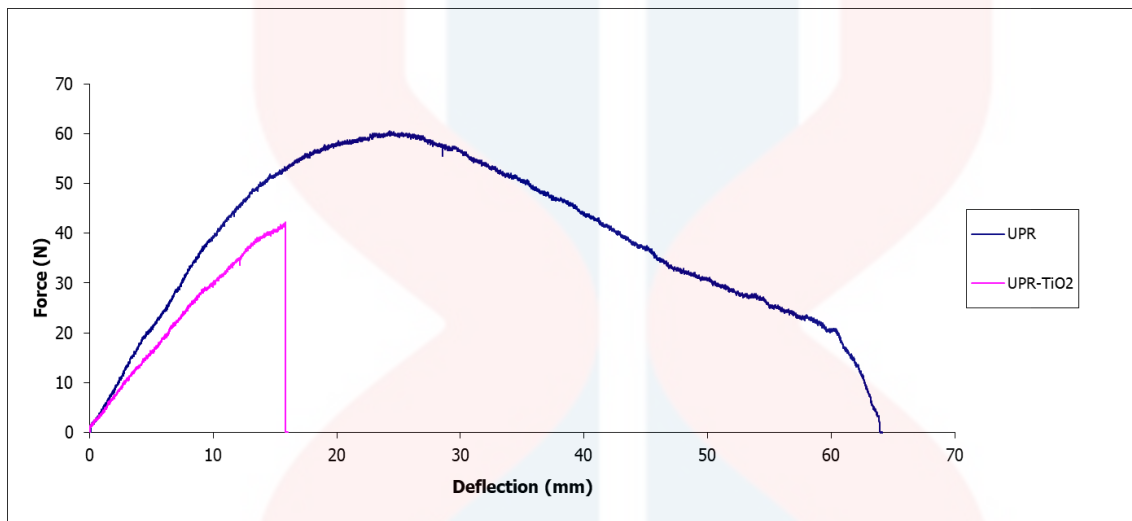


Figure 4.12: Bending strength of UPR and UPR-TiO<sub>2</sub> composite

Figure 4.13 depicts the bending strength of the UPR-DGISF-TiO<sub>2</sub> composites. The highest bending strength was observed for UPR-DGISF-TiO<sub>2</sub> composite having 25wt% DGIF. This composite indicates that the incorporation TiO<sub>2</sub> particles into UPR-DGISF creates composite with good tensile (Figure 4.10) and bending strength. The second flexible composite was UPR-20wt%DGIF-1wt%TiO<sub>2</sub> and followed by the UPR-30wt%DGIF-1wt%TiO<sub>2</sub> composite. The composite containing 30wt% DGIF with 1wt% TiO<sub>2</sub> has shown significant reduction on bending strength. This is because the presence of a high amount of DGIF dominantly contributes to the final composite properties.

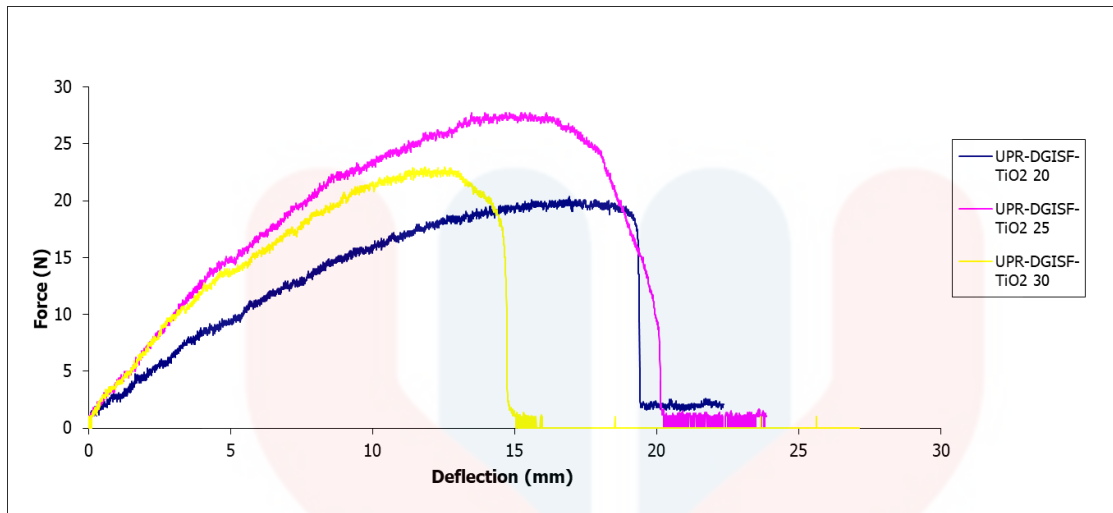


Figure 4.13: Bending strength of UPR-DGISF-TiO<sub>2</sub> composites

#### 4.4.3 Hardness

The hardness of the UPR, UPR-TiO<sub>2</sub>, UPR-DGISF and UPR-DGISF-TiO<sub>2</sub> composites were tested using Shore D durometer by determining the depth of an indentation in the material under test. Figure 4.14 shows the variation of hardness UPR, UPR-TiO<sub>2</sub>, UPR-DGISF and UPR-DGISF-TiO<sub>2</sub> composites. The highest hardness is UPR containing 30 wt% of DGIF. The structural integrity of a material and the resistance of its components to deformation determine its hardness. DGIF can help to make a composite stiffer and, resulting in greater hardness. The addition of TiO<sub>2</sub> slightly reduced the hardness of UPR-DGISF composites. The presence of TiO<sub>2</sub> was regarding to more well-structured composite as a result of its more uniformly embedded in UPR matrix, which shown by SEM images (Figure 4.7).

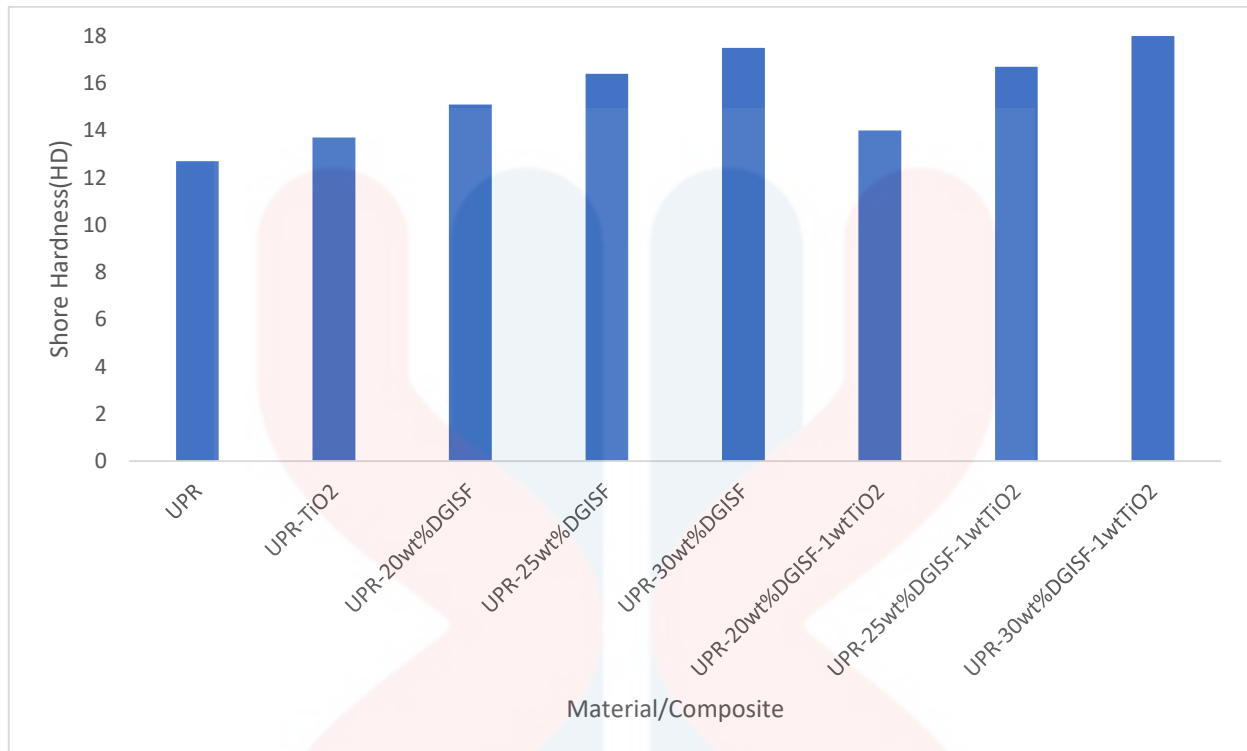


Figure 4.14: Shore D hardness of neat UPR, UPR-TiO<sub>2</sub>, UPR-DGISF and UPR-DGISF-TiO<sub>2</sub> composites

## CHAPTER 5

### CONCLUSIONS AND RECOMMENDATIONS

#### 5.1 Conclusions

This study was successfully developed the UPR-DGISF composite with  $\text{TiO}_2$  addition. Adding  $\text{TiO}_2$  to UPR-*Donax Grandis* fiber composites has been demonstrated to have a considerable impact on UPR-DGISF characteristics.

Different amount of DGIF in the UPR matrix had influence the overall performance of the composites. The composite with 25wt% DGIF has better tensile strength and bending strength while 30wt% has better hardness compared to the composite with 20wt%. They exhibit better and uniform interfacial adhesion of embedded DGIF in UPR matrix which was shown by SEM images. It is worth noting that all the composites have corresponding functional groups, which indicates that they have comparable chemical compositions.

The addition of  $\text{TiO}_2$  particles in UPR-DGISF composites also produced high tensile strength, bending strength, and hardness. The composite with 25wt% DGIF had shown greatly better mechanical properties with addition of 1wt%  $\text{TiO}_2$  among other composites.  $\text{TiO}_2$  particles could potentially aid in achieving a more uniform distribution and interaction between DGIF and UPR. The composite with lower content of DGIF (20wt%) is more prone to be brittle than the composite with higher content of DGIF (25 and 30 wt%). Overall, the incorporation of a blend of UPR, DGIF, and  $\text{TiO}_2$  in a specific ratio allows for a synergistic effect, whereby the

individual components complement each other, resulting in a composite material that exhibits desirable mechanical properties.

## 5.2 Recommendations

This study has made major advances in understanding the impacts of TiO<sub>2</sub> addition on UPR-DGISF composites, there are various areas for future research to investigate such as TiO<sub>2</sub> content optimization and interaction mechanism, processing parameter and durability studies. In order to achieve a composite matrix with enhanced performance and cost-effectiveness, it is essential to determine the most suitable concentration of TiO<sub>2</sub>. By careful evaluation of different concentrations, the optimal amount can effectively balance both cost and performance. Moreover, more research to modify TiO<sub>2</sub> particle surfaces to enhance compatibility with UPR matrix and improve overall.

A thorough investigation of the effects of processing factors such as temperature, pressure, and curing time is essential. This research will provide valuable insights into ways to improve the quality and reliability of these composites and contribute to the advancement of composite material technology. It is also recommended to conduct long-term durability tests to assess the stability and resilience of TiO<sub>2</sub>-reinforced polymer composites under various environmental conditions such as moisture, UV radiation, and temperature variations. Future research can increase our understanding of TiO<sub>2</sub> reinforced UPR-*Donax Grandis* fibre composites and allow their widespread implementation in a variety of industrial applications by addressing these research objectives.

## REFERENCES

Admin. (2022). Synthetic and Natural Fibres - Definition, Examples, Types, Advantage, Videos and FAQs of Synthetic and Natural. *BYJUS*. <https://byjus.com/chemistry/synthetic-natural-fibres/>

Builes, D. H., & Tercjak, A. (2019). Microscopic analysis of unsaturated polyester Resin-Based composites and nanocomposites. In *Elsevier eBooks* (pp. 275–311). <https://doi.org/10.1016/b978-0-12-816129-6.00013-2>

Cazan, C., Enesca, A., & Andronic, L. (2021). Synergic Effect of TiO<sub>2</sub> Filler on the Mechanical Properties of Polymer Nanocomposites. *Polymers*, 13(12), 2017. <https://doi.org/10.3390/polym13122017>

Enescu, D., Dehelean, A., Gonçalves, C., Vicente, A. A., Magdas, D. A., Fuciños, P., & Cerqueira, M. A. (2020b). Evaluation of the specific migration according to EU standards of titanium from Chitosan/Metal complexes films containing TiO<sub>2</sub> particles into different food simulants. A comparative study of the nano-sized vs micro-sized particles. *Food Packaging and Shelf Life*, 26, 100579. <https://doi.org/10.1016/j.fpsl.2020.100579>

Girijappa, Y. G. T., Sanjay, M. R., & Siengchin, S. (2019). Natural Fibers as Sustainable and Renewable Resource for Development of Eco-Friendly Composites: A Comprehensive Review. *Frontiers in Materials*, 6. <https://doi.org/10.3389/fmats.2019.00226>

Julius, N. L. H. S. & A. (2022, October 14). *Donax canniformis* (G.Forst.) K.Schum.(Marantaceae). *Malaysia Biodiversity Information System (MyBIS)*. <https://www.mybis.gov.my/art/431>

Kong, I. (2022). Properties of bio-based fibers. In *Elsevier eBooks* (pp. 33–64)

.<https://doi.org/10.1016/b978-0-12-824543-9.00027-x>

Libretexts. (2020, November 3). *Infrared Spectroscopy Absorption Table*. Chemistry LibreTexts.

[https://chem.libretexts.org/Ancillary\\_Materials/Reference/Reference\\_Tables/Spectroscopic\\_Reference\\_Tables/Infrared\\_Spectroscopy\\_Absorption\\_Table](https://chem.libretexts.org/Ancillary_Materials/Reference/Reference_Tables/Spectroscopic_Reference_Tables/Infrared_Spectroscopy_Absorption_Table)

Mahltig, B. (2018). Cellulosic-Based Composite Fibers. In *Inorganic and Composite Fibers*.<https://doi.org/10.1016/b978-0-08-102228-3.00013-x>

Mann, G., Azum, N., Asiri, A. M., Rub, M. A., Hassan, M. I., Fatima, K., & Asiri, A. M. (2023). Green Composites Based on Animal Fiber and Their Applications for a Sustainable Future. *Polymers*, 15(3), 601. <https://doi.org/10.3390/polym15030601>

Ong, H. C. (2004). *Tumbuhan liar: khasiat ubatan & kegunaan lain*. Utusan Publications.

Prasad, V., Joseph, M., & Sekar, K. (2018). Investigation of mechanical, thermal and waterabsorption properties of flax fibre reinforced epoxy composite with nano TiO<sub>2</sub> addition. *Composites Part A-applied Science and Manufacturing*, 115, 360–370. <https://doi.org/10.1016/j.compositesa.2018.09.031>

Saba, N., Jawaid, M., & Sultan, M. T. H. (2019). An overview of mechanical and physical testing of composite materials. In Elsevier eBooks (pp. 1–12). <https://doi.org/10.1016/b978-0-08-102292-4.00001-1>

Qin, C., Jin, Q., Zhao, J., Wang, Y., & Jiang, C. (2023). Study on the mechanical characteristics, heat resistance, and corrosion resistance of unsaturated polyester resin composite. *Buildings*, 13(7), 1700. <https://doi.org/10.3390/buildings13071700>

## APPENDIX A

Table A1: Tensile strength of UPR-DGISF-TiO<sub>2</sub> composites.

Test No	Youngs Modulus (N/mm <sup>2</sup> )	Stress @ Peak (N/mm <sup>2</sup> )	Stress @ Yield (N/mm <sup>2</sup> )	Stress @ Break (N/mm <sup>2</sup> )	Strain @ Break (%)	Force @ Peak (N)
TiO2 20	753.061	9.378	9.378	0.577	2.066	497.400
TiO2 25	641.271	8.946	8.946	0.285	2.107	537.000
TiO2 30	687.948	8.140	8.140	0.139	2.006	486.300
Min	641.271	8.140	8.140	0.577	2.006	486.300
Mean	694.093	8.821	8.821	0.241	2.060	506.900
Max	753.061	9.378	9.378	0.139	2.107	537.000
S.D.	56.148	0.628	0.628	0.360	0.051	26.652
C. of V.	8.089	7.120	7.120	149.386	2.456	5.258
L.C.L.	554.613	7.261	7.261	-1.135	1.934	440.693
U.C.L.	833.574	10.381	10.381	0.653	2.186	573.107

Table A2: Tensile strength of UPR-DGISF composites

Test No	Youngs Modulus (N/mm <sup>2</sup> )	Stress @ Peak (N/mm <sup>2</sup> )	Stress @ Yield (N/mm <sup>2</sup> )	Stress @ Break (N/mm <sup>2</sup> )	Strain @ Break (%)	Force @ Peak (N)
1	366.057	6.773	6.773	-0.191	3.250	376.700
2	642.071	7.449	7.449	0.041	1.713	416.300
3	600.948	6.502	6.502	-0.643	1.460	380.500
Min	366.057	6.502	6.502	-0.643	1.460	376.700
Mean	536.358	6.908	6.908	-0.264	2.141	391.167
Max	642.071	7.449	7.449	0.041	3.250	416.300
S.D.	148.912	0.487	0.487	0.348	0.969	21.849
C. of V.	27.764	7.057	7.057	-131.712	45.262	5.586
L.C.L.	166.437	5.697	5.697	-1.128	-0.266	336.890
U.C.L.	906.280	8.119	8.119	0.600	4.548	445.443

Table A3: Tensile strength of UPR and UPR-TiO<sub>2</sub> composite

Test No	Youngs Modulus (N/mm <sup>2</sup> )	Stress @ Peak (N/mm <sup>2</sup> )	Stress @ Yield (N/mm <sup>2</sup> )	Stress @ Break (N/mm <sup>2</sup> )	Strain @ Break (%)	Force @ Peak (N)
1	766.535	36.280	36.280	-1.082	6.815	2125.300
2	1078.990	21.698	21.698	-0.957	2.984	1195.100
Min	766.535	21.698	21.698	-1.082	2.984	1195.100
Mean	922.762	28.989	28.989	-1.020	4.899	1660.200
Max	1078.990	36.280	36.280	-0.957	6.815	2125.300
S.D.	220.939	10.312	10.312	0.089	2.709	657.751
C. of V.	23.943	35.571	35.571	-8.703	55.300	39.619
L.C.L.	-1062.294	-63.657	-63.657	-1.817	-19.444	-4249.454
U.C.L.	2907.818	121.635	121.635	-0.222	29.242	7569.854

Table A4: Flexural strength of UPR and UPR-TiO<sub>2</sub> composite

Test No	Bending Modulus (N/mm <sup>2</sup> )	Bending Strength @ Peak (N/mm <sup>2</sup> )	Force @ Peak (N)	Bending Strength @ Yield (N/mm <sup>2</sup> )
1	1571.649	46.749	60.500	10.586
2	1849.952	43.200	42.200	8.906
Min	1571.649	43.200	42.200	8.906
Mean	1710.801	44.974	51.350	9.746
Max	1849.952	46.749	60.500	10.586
S.D.	196.790	2.510	12.940	1.188
C. of V.	11.503	5.580	25.200	12.189
L.C.L.	-57.289	22.425	-64.912	-0.927
U.C.L.	3478.890	67.523	167.612	20.420

Table A5: Bending strength of UPR-DGISF composites at different compositions

Test No	Bending Modulus (N/mm <sup>2</sup> )	Bending Strength @ Peak (N/mm <sup>2</sup> )	Force @ Peak (N)	Bending Strength @ Yield (N/mm <sup>2</sup> )
1	618.331	14.855	14.800	2.911
2	1224.030	20.071	21.400	4.033
3	1453.175	19.789	21.100	4.033
Min	618.331	14.855	14.800	2.911
Mean	1098.512	18.238	19.100	3.659
Max	1453.175	20.071	21.400	4.033
S.D.	431.343	2.933	3.727	0.648
C. of V.	39.266	16.084	19.513	17.706
L.C.L.	26.984	10.951	9.842	2.049
U.C.L.	2170.040	25.525	28.358	5.268

Table A6: Flexural strength of UPR-DGISF-TiO<sub>2</sub> composites

Test No	Bending Modulus (N/mm <sup>2</sup> )	Bending Strength @ Peak (N/mm <sup>2</sup> )	Force @ Peak (N)	Bending Strength @ Yield (N/mm <sup>2</sup> )
1	1020.628	22.081	20.400	4.221
2	1483.759	23.753	27.700	5.316
3	1606.314	19.818	23.000	4.050
Min	1020.628	19.818	20.400	4.050
Mean	1370.234	21.884	23.700	4.529
Max	1606.314	23.753	27.700	5.316
S.D.	308.906	1.975	3.700	0.687
C. of V.	22.544	9.024	15.612	15.173
L.C.L.	602.860	16.978	14.509	2.822
U.C.L.	2137.607	26.790	32.891	6.236

## APPENDIX B

Table 4.1: hardness of UPR and UPR-TiO<sub>2</sub>

Test point Name	1	2	3	4	5	Average value
UPR	13.5	13	14.5	11	11.5	12.7
UPR-TiO <sub>2</sub>	13	14.5	12.5	13	15.5	13.7

Table 4.2: hardness of UPR-DGISF-TiO<sub>2</sub>

Test point Name	1	2	3	4	5	Average value
UPR-DGISF- TiO <sub>2</sub> 20	14.5	14.5	15.5	15	16	15.1
UPR-DGISF- TiO <sub>2</sub> 25	17	16	15.5	16	17.5	16.4
UPR-DGISF- TiO <sub>2</sub> 30	16.5	17.5	20	16.5	17	17.5

Table 4.3: hardness of UPR-DGISF 20, UPR-DGISF 25, UPR-DGISF 30

Test point Name	1	2	3	4	5	Average value
UPR- DGIF 20	14.5	14.5	16	12	13	14
UPR- DGIF 25	18	19	17.5	15	14	16.7
UPR- DGIF 30	17	17.5	19.5	17	19	18